Response file to comments

Reviewer #1

1. It seems that the main question the authors are answering ("what are the difference between an entrainment form conservation equation and when to use a flux-based formulation") rather is "When does a modeler need to properly account for suspended load mechanisms?"

We have rephrased the questions, and their order in the new manuscript. They now more closely reflect the reviewer's comments. See Lines 100-105 of the manuscript with track changes.

2. The authors treat the flux form of the mass conservation equation as a synonym to a capacity-based or equilibrium approach, and the entrainment form of the mass conservation equation is considered noncapacity-based or non-equilibrium. I think the two types of models (flux form and entrainment form) are not synonyms for capacity-based and noncapacity-based. These terms are not equivalent. Revising this may impact several parts of the text.

We have now specifically defined what we mean by the flux form and entrainment form. See Lines 23-24 of the manuscript with track changes. We define again here: "Here we identify the flux form as based on the local capacity sediment transport rate, and the entrainment form as based on the local capacity entrainment rate". Although we do not go into details in the paper, we note here that our system (the Yellow River) is suspension-dominated to the point where bedload is negligible. The phenomenon documented by Bell and Sutherland (1983) can be quantified using an entrainment-based *bedload* formulation such as Pelosi and Parker (2014). We note here that El kadi Abderrezzak and Pacquier (2009) list the form $dQ_s/dx = (Q_s^{cap} - Q_s)/L_{ad}$. where L_{ad} is the adaptation length. This is nothing more and nothing less than an entrainment form, but one for which the guts of the adaptation length L_{ad} remain undefined. In our system L_{ad} is specifically given as $q_w/(v_s r_0)$, where q_w is the water discharge per unit width and v_s is fall velocity.

3. Associated with the previous comment: Could Bell and Sutherland (1983) and Armanini and Di Silvio (1988) be examples of the flux-form combined with a non-capacity approach?

Bell and Sutherland (1993) is by and large a bedload entrainment formulation with an extra term. See their Eq. (14) therein. The term g_{se} denotes the locally-computed capacity transport rate. Armanini and Di Silvio (1988) is complex and hard to interpret.

4. Associated with the same comment: And may Blom and Parker (2004), Blom et al. (2006, 2008) be an example of the entrainment form combined with a capacity-based approach?

We are happy to reply, "yes!" They have the distinguishing feature of, you guessed it, eliminating the need for an active layer!

5. Isn't the Exner equation of conservation of sediment mass a flux-based approach? Shouldn't the authors consider another (other than "Exner") name for the entrainment form of conservation of sediment mass?

The flux form of Exner is:

$$\left(1-\lambda_p\right)\frac{\partial \eta}{\partial t}=-\frac{\partial q_s}{\partial x}$$

The entrainment form is:

$$\left(1-\lambda_p\right)\frac{\partial \eta}{\partial t}=-v_s\left(E-r_oC\right)$$

$$\frac{\partial Ch}{\partial t}+\frac{\partial q_s}{\partial x}=v_s\left(E-r_oC\right)$$

The first and second equations above are alternative forms for sediment mass conservation (Exner). We have not modified the paper in this regard. The third equation can be written as,

$$\frac{\partial Ch}{\partial t}+\frac{\partial q_s}{\partial x}=\frac{1}{L_{ad}}\left(q_{se}-q_s\right) \quad , \quad q_{se}=\frac{E}{r_o}q_w \quad , \quad L_{ad}=\frac{q_w}{r_o v_s}$$

Thus it fits within the generic form below, which can be found in Bell and Sutherland (1983) and El kadi Abderrezzak and Paquier (2009).

$$???+\frac{\partial q_s}{\partial x}=\frac{1}{L_{adapt}}\left(q_{se}-q_s\right)$$

We have not modified the text: both papers are already quoted in the text.

6. Ln 26 "study this problem by comparing the results of flux-based and entrainment-based morphodynamics". Please explain in what way you are comparing the two types of conservation models. This also holds for ln 105-106. One of the ways seems to be by mimicking "the reduction of the sediment load in the LYR in recent years" (Ln 279). I think this information needs to be moved to the Introduction section. Figs 6 and 7. Shouldn't the equilibrium channel slope and bed surface texture be equal for the flux form and the entrainment form? It would be nice if the authors would confirm this.

The reviewer is right that the comparison is conducted based on the premise of a reduction of sediment supply, so as to mimic the effect of the operation of Xiaolangdi Dam. We have explained this in the manuscript. See Line 30 and Lines 108-109 of the manuscript with track changes.

In terms of the channel equilibrium predicted by the flux and the entrainment forms, actually we have explained this in Section 4.3 in the original manuscript. See Lines 609-611 of the manuscript with track changes.

7. Ln 26 "study this problem by comparing the results of flux-based and entrainment-based morphodynamics under conditions typical of the Lower Yellow River". I would suggest to develop generic guidelines for when to use an entrainment form conservation equation and when to use a flux-based formulation, and only after this move toward the case of the Lower Yellow River.

While we have not performed a general study, we have performed the calculations for the evaluation requested by the reviewer. In Line 522 of the manuscript with track changes, we point out that the adaptation length L_{ad} for uniform material is only 1.88 km, a value that is small compared to the reach length of 200 km. We identify this as the reason that the flux formulation can be used; i.e. $L_{ad}/L << 1$. We also show that this condition does not holds for the finer sizes typical bed material of the Yellow River. We have modified a sentence to read "In this case and in general, the predictions of the flux form and the entrainment form show little difference when $L_{ad}/L << 1$, where L is domain length." See Lines 523-524 of the manuscript with track changes.

8. Ln 45-47. I'd rephrase this as application of the entrainment form of the conservation equation is not necessarily limited to suspended sediment.

The sentence has been rephrased so that the entrainment form is not limited to suspended sediment. See Lines 50-51 of the manuscript with track changes.

9. Ln 57-71. These lag issues are not only covered by the entrainment form, but may also be covered by the flux form… Also see comment 2.

We do not think so. As we have described in response to Query 2, we believe that *all* formulations of the form $dQ_s/dx = (Q_s^{cap} - Q_s)/L_{ad}$ are entrainment forms, in which the entrainment rate ~ Q_s^{cap}/q_w. Again, this holds regardless of whether the mode of transport is bedload or suspended load.

10. Ln 78. "More recently, however, since the operation of Xiaolangdi Dam in 1999 the LYR has seen a substantial reduction in its sediment load (Fig. 1(b))". - The authors do not address the distinct temporal decrease of the annual sediment load between 1950-2000. - Why is the year 2000 indicated in Figure 1b and not 1999? Please indicate in the figure whether 2000 is supposed to indicate the year of the Xiaolangdi Dam construction.

The reviewer is right that there is a typo in Figure 1(b). The year 1999, rather than 2000, should be used which indicates the time of the operation of the Xiaolangdi Dam. The figure has been replotted as suggested by the reviewer. We have also rephrased the sentence so that the decrease of sediment load in recent decades is addressed. See Line 82 of the manuscript with track changes.

11. Figure 1 shows a number of very interesting features that are currently not addressed by the authors: - the distinct temporal decrease of the annual sediment load between 1950-2000. What is the cause of this decrease? - The three lines for the three cities are highly correlated. Please indicate and explain. - The suspended load is significantly finer than the bed material (i.e., grain size selective transport) – Does the "bed material" consider the bed surface or substrate? Please specify. - The bed material nicely shows downstream fining. Please explain. Is this due to preferential deposition of coarse sediment or particle abrasion? Or a combination?

(1) The decrease in sediment load prior to 2000 is a basinwide phenomenon that is not directly

germane to this paper. We can understand why the issues caught the eye of the reviewer. We consulted our co-author, Yuanfeng Zhang, who is perhaps the foremost (in China and thus the world) expert on sediment transport in the Yellow River. This is what he said. "There are 3 main reasons for the sediment load decrease from 1970 (strictly say is that from 1980s for the LYR) to 2000: (a) revegetation, (b) terrace fields, (c) checkdam and small dam (we saw lots of them in 2017), and also other reasons such as taking sediment from river for construction, climate changes etc." We have not added this to the paper, as we do not wish to focus on basinwide sediment production.

(2) Of the three lines for load, note that there is a consistent decline from Huayuankou (upstream) to Lijin (downstream). This is consistent with a river in depositional mode in the giant alluvial fan of the North China Plain.

(3) We are not aware of any studies of the abrasion of silt in water. The particles are likely too fine to undergo comminution due to collision.

12. I'd change the order of the research questions in Ln 94-96 "Is the entrainment formulation really necessary when modeling the LYR? Or more specifically, under what circumstances should a numerical modeler be impelled to implement the entrainment formulation instead of the flux formulation for river morphodynamic modeling?" to 1. "Under what conditions should one apply an entrainment form or flux form description of conservation of sediment mass?" 2. "Which form of the sediment conservation equation is most suitable for LYR?"

The research questions have been rephrased according to the suggestion of the reviewer. See Lines 100-105 of the manuscript with track changes.

13. Ln 118. No bedrock. Please explain to the reader how valid this assumption is.

We again consulted Yuanfeng Zhang about this. "The LYR has been heavy sediment-laden and depositional river for hundreds or thousands years. So, definitely, no exposed bedrock in the LYR". We have modified the text. See Lines 131-132 of the manuscript with track changes.

14. Ln 119. I think here you say that you impose a constant flow rate and sediment supply rate at the upstream end. What impact does this assumption have on the model results and conclusions? Please address this in the discussion section. Also holds for Lines 133-137.

We present numerical cases with hydrographs in the new Supplement. Results indicate that our conclusions based on constant flow discharge also hold when hydrographs are implemented. See Section S2 and S3 of the Supplement.

We have also moved Appendix A and Appendix B to the Supplement.

15. Ln 164 or Eq.7. It is about the interface elevation and not the bed surface elevation. The parameter La is missing. Right-hand terms should read d(zb-La)/dt<0 and d(zb-La)/dt>0.

The reviewer is right that $d(z_b\text{-}L_a)$, rather than dz_b, should be used in the right-hand terms. But since a constant active layer thickness L_a is implemented in this paper, the two forms are identical. We have revised the equation as suggested by the reviewer, so that it is more universal.

16. Ln 226-230. The friction term in the original E&H formulation includes form drag. If there is barely any form drag such as in the LYR, then it makes sense that the original E&H does not do well and needs to be adjusted.

We agree with the reviewer. Actually we think that the lack of form drag in the LYR leading to very high sediment transport rates, which cannot be reproduced by the original E&H formulation. We quote Ma et al. (2017) in this regard.

17. Ln 232-247. It may be interesting to mention that a fractional version of E&H was first proposed by Van der Scheer et al. (2002) and was later used by Blom et al. (2016, 2017a, 2017b).

We have added the references. See Lines 274-276 of the manuscript with track changes.

18. Ln 310. Please be specific. "Slower degradation" refers to a slower downstream propagation of the degradational wave? Differences between Figs 3a and 4a are difficult to see anyway.

We have added insets in Figure 3-8 to show the detailed results of the bed elevation near the upstream end. A comparison between Figure 3(a) and Figure 4(a) shows that the flux form predicts a 3 m degradation at the upstream end whereas the entrainment form predicts a 2.3 m degradation. This is the reason why we say "slower degradation". See Lines 341-342 of the manuscript with track changes.

19. Ln 310. "more diffusive sediment load reduction". Or a faster downstream propagation of the disturbance?

We think that they are the same thing.

20. Ln 342. 0.05. Why so extreme? Ln 483. 20. Why so extreme?

These intentionally extreme values allow us to explore limiting behavior. The reason for choosing extreme values is to understand under what conditions the flux form and the entrainment form lead to different/similar predictions, as explained in the manuscript. We have specifically demonstrated that such values are unrealistic. See Line 381 and Line 461 of the manuscript with track changes.

21. Ln 363-364. "The sediment supply rate of each grain size range is set at 10% of its equilibrium sediment transport rate. This results in… and a grain size distribution of the sediment supply… that is identical to the grain size distribution of the equilibrium sediment load." Here it is essential for the reader to understand that the GSD of the sediment supply does not change: only the total sediment supply is reduced by 90%. This means that also the equilibrium GSD of the suspended load must be the same as the one of the sediment supply and so does not change with time. The equilibrium bed surface texture gets coarser with a reduction of the total sediment supply (Blom et al. 2016, 2017a). This is because with a reduced total sediment supply the equilibrium flow velocity

decreases and the mobility difference between the grain size fractions increases. This implies that with a decrease of the total sediment supply the bed surface needs to coarsen to allow for the supplied sediment to be transported downstream. These things need to be explained to the reader.

We have explained in the manuscript that the GSD of the sediment supply does not change and only the total sediment supply is reduced by 90%. See Lines 411-412 of the manuscript with track changes. As for the surface coarsening, we have added the following line to the text. "This represents armoring, mediated by the hiding functions of Eqs. (26) and (27)." See Lines 423-424 of the manuscript with track changes.

22. Ln 372. "with at least two kinematic waves". Each grain size fraction induces the migration of a perturbation (Stecca et al., 2014, 2016). It would be nice to illustrate this.

The two reference should have been in the original text. They have now been added to the manuscript. See Lines 418-419 of the manuscript with track changes. By way of apology, we mention that Stecca (2014) is referenced copiously in our recent paper below.

An, C-G., Fu, X-D., Wang, G-Q and Parker, G. 2017. Effect of Grain Sorting on Gravel-bed River Evolution Subject to Cycled Hydrograph: Bedload Sheets and Breakdown of the Hydrograph Boundary Layer. Journal of Geophysical Research, 122(8), 1513-1533, DOI: 10.1002/2016JF003994.

23. Ln 376. See previous two comments. I think it would be illustrative and helpful if the authors would validate whether, if they continue their runs for a very long time, the GSD of the suspended load becomes equal to the GSD of the sediment supply.

In Section 4.3 we have demonstrated that under equilibrium condition, the sediment transport rate of each grain size equals to the sediment supply rate of each grain size. This statement indicates that the GSD of suspended load equals the GSD of sediment supply. See Lines 609-611 of the manuscript with track changes.

24. Ln 438. The authors neglect the temporal derivative. Can the authors quantify or justify this assumption?

We neglect the temporal derivative with the purpose to simplify the mathematical analysis and characterize the adaptation length scale (rather than the adaptation time scale). The adaptation time scale can be obtained if we neglect the spatial derivative and conduct a similar analysis. We explain this in the manuscript. See Line 498 of the manuscript with track changes.

25. Figs 6 and 7. Shouldn't the equilibrium channel slope and bed surface texture (Blom et al, 2017a) be equal for the flux form and the entrainment form? It would be nice if the authors would confirm this.

Yes, we have confirmed this in Section 4.3. See Lines 609-611 of the manuscript with track changes.

26. Section 3.2. Has the value of the active layer thickness been provided, and the total number of grain size fractions n? What is the height of the grid cells used to register the surface and substrate GSD? The flow is solved using a Godunov type scheme. What about the conservation equations for sediment mass? How are they solved?

The value of active layer thickness (L_a = 0.738) was provided at the beginning of Section 3. See Line 296 of the manuscript with track changes. The total number of grain size fractions can be inferred from Figure 2: n = 5. We have added this information to the text. See Line 305 of the manuscript with track changes. The height of grid cell to register the surface GSD is L_a. The height to register the substrate GSD is 0.5 m. This information has been added to the text. See Line 297 of the manuscript with track changes. For the conservation equations for sediment mass, we implemented a first-order explicit scheme for the temporal derivatives and a first-order upwinded scheme for the spatial derivatives.

27. The authors mention that they fix the downstream bed elevation by assuming normal flow at the downstream end. Yet, later the authors seem to mention that actually they put the downstream boundary condition sufficiently far to avoid backwater effects. Isn't this a contradiction?

If we put the downstream boundary condition close to the river mouth, the backwater effects would be so strong that the normal flow assumption would not be appropriate. Therefore, we put the downstream boundary sufficiently far upstream of the mouth so that the normal flow can be implemented as the downstream boundary condition.

28. In the simulation results one observes that changes in grain size arrive at the downstream end although bed elevation is constant with time. I do not understand this.
HERE

The active layer is taken to be 0.738 m in thickness. It adjusts much more quickly than bed elevation itself. You will find the same result in:

An, C-G., Fu, X-D., Wang, G-Q and Parker, G. 2017. Effect of Grain Sorting on Gravel-bed River Evolution Subject to Cycled Hydrograph: Bedload Sheets and Breakdown of the Hydrograph Boundary Layer. Journal of Geophysical Research, 122(8), 1513-1533, DOI: 10.1002/2016JF003994.

29. Has the CFL criterion for modelling bed elevation and the flow been considered?

The CFL criterion has been considered such that that the time steps implemented in the simulation are small enough to avoid numerical instabilities.

30. Section 3.2. Have the authors experienced any unreasonable instabilities in their numerical runs (Chavarrias et al, 2018)?

Even though Chavarrias et al. (2018) has reported that unreasonable instabilities could occur

under certain circumstances when modeling mixed sediment river morphodynamics, we did not run into such problems in our simulations. We have mentioned this in the manuscript. See Lines 673-675 of the manuscript with track changes.

31. Figure 9. The adaptation length is represented by 3-4 cells. Could the conclusion that the adaptation is irrelevant be due to not well solving it?

In order to check whether the adaptation is irrelevant be due to poorly solving for it, we recalculated the case of uniform sediment (in Section 3.1) with a smaller cell size. The cell size specified here is Δx = 250 m, which is half the cell size specified in the manuscript. Figure R1 and Figure R2 show the modeling results using the flux form and the entrainment form of the Exner equation, respectively.

If we compare Figure R1 with Figure 3 in the MS, and Figure R2 with Figure 4 in the MS, we can see that reducing the cell size from 500 m to 250 m has almost no influence on the simulation results, in terms of both the flux form and the entrainment form of the Exner equation. So we think that our solution might be pretty good!

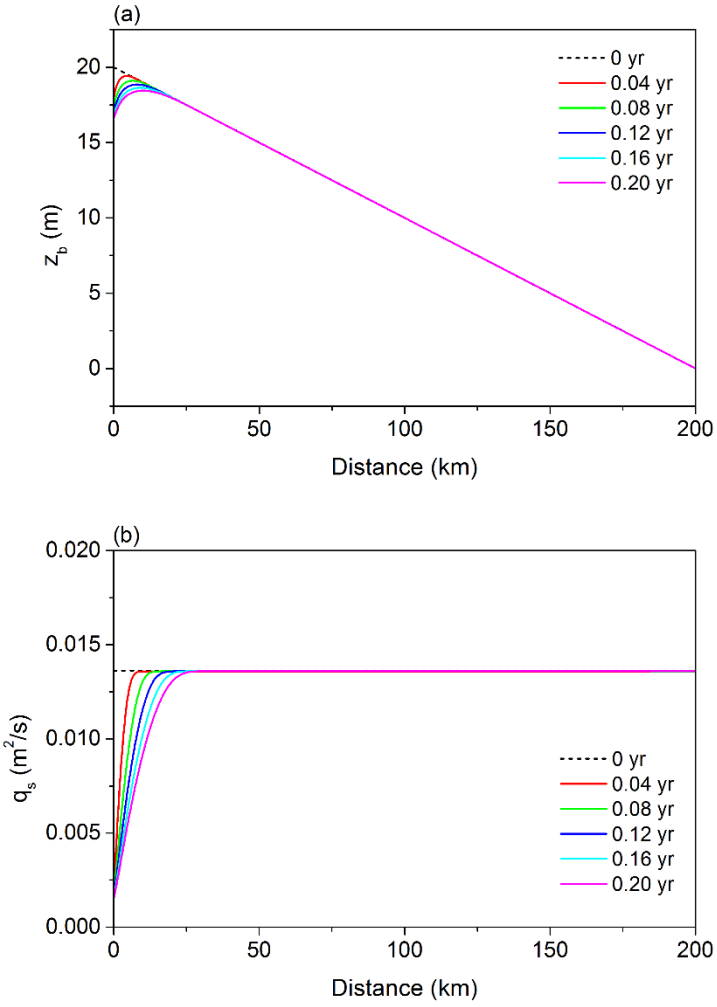

Figure R1. Case of uniform sediment using the flux form of Exner equation and a cell size of 250 m (half of that implemented in the MS). Time variation of (a) bed elevation z_b and (b) sediment

load per unit width q_s in response to the cutoff of sediment supply.

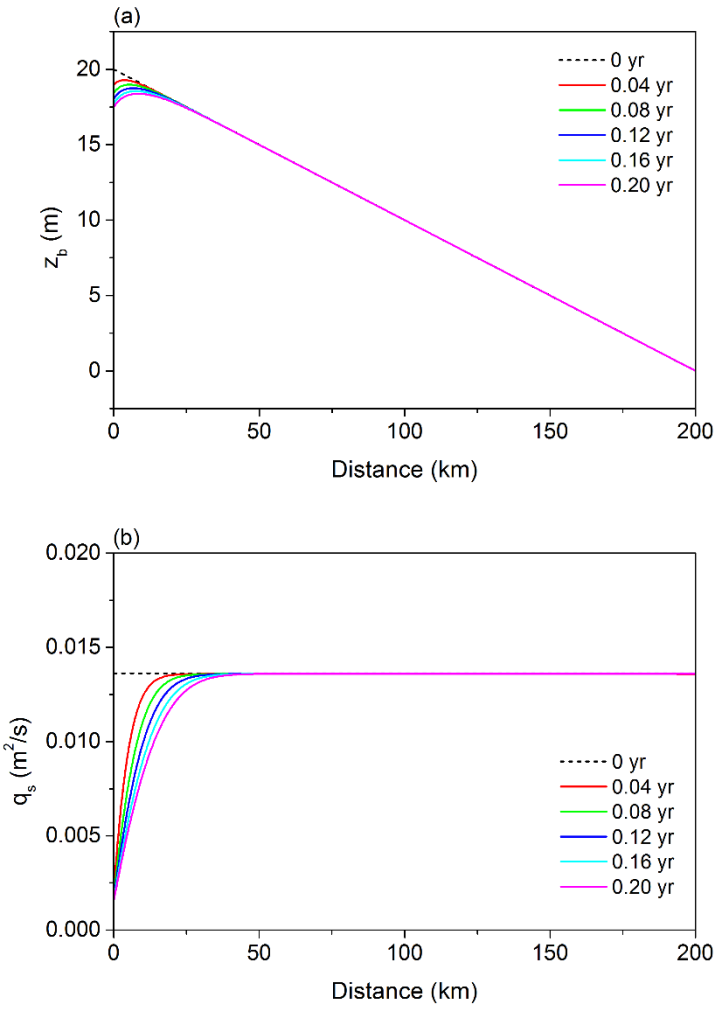

Figure R2. Case of uniform sediment using the entrainment form of Exner equation and a cell size of 250 m (half of that implemented in the MS). Time variation of (a) bed elevation z_b and (b) sediment load per unit width q_s in response to the cutoff of sediment supply.

32. Section 4.2. I think the authors may like to consider these results in the context of the results of Stecca et al (2014, 2016).

The papers of Stecca et al. (2014, 2016) should have been referenced in the original manuscript. They are now referenced in the new manuscript. See Lines 560-562 of the manuscript with track changes.

33. Equation (37). The authors treat only one fraction and consider the equation to be an advection equation. In reality they have a system of advection equations in which the source terms links them. This may yield different behavior.

We think that in Section 4.2 we actually treat the equation system rather than only one equation, because Eq. (37) holds for each size fraction. If we list i from 1 to n-1, we get the equation system.

But here we only show the general formulation of the equation system, which is enough to explain our modeling results. As for the interaction among different size fractions, it is represented in the source term of Eq. (39) via the terms with subscription j ($j \neq i$).

34. Equation (38). The authors are not the first ones. I think the authors should compare these results to the ones of Stecca (2014, 2016).

The reviewer is right that we are not the first ones to study this problem. The mathematical analysis of Stecca et al. (2014, 2016) is a bit different form our analysis in that they implemented the St. Venant equation as well as a linearized analysis which is only applicable for small perturbations. But the overall characteristics of the governing equations derived by Stecca et al. (2014, 2016) and this paper are similar. Since the purpose of the mathematical analysis in this section is to explain the modeling results in Section 3, we do not think that it is necessary to compare our analysis with that of Stecca et al. (2014, 2016) in detail at this point in the paper. We have, however, referenced Stecca et al. (2014, 2016) and related papers in the new manuscript. See Lines 560-562 of the manuscript with track changes.

35. Lines 494-498: I'd propose to rephrase.

We have slightly reworded the text. See Lines 555-560 of the manuscript with track changes.

36. Line 557-558. The authors say the entrainment form is needed when studying sorting processes. I do not think this conclusion can be drawn.

We appreciate the reviewer for the correction. Actually what we want to say is that the entrainment form is needed when studying the sorting processes of fine-grained sediment. This is because fine-grained sediment has a large adaptation length L_a and a large diffusivity coefficient ν_i. The flux form can lead to an overestimation of advection as it pertains to sorting processes under such circumstances. We have revised the text to make our statement more clear. See Lines 618-634 of the manuscript with track changes.

37. The conclusion section reads as a summary. I'd recommend revision and limiting the section to conclusions.

We have rephrased the Conclusion a bit. Generally we prefer the Conclusion the way it is.

38. Ln 643-646. Is the entrainment form recommended provided that all 3 requirements are fulfilled or if only 1 of the 3 is fulfilled?

We have revised the text to make our conclusion clear. In the new text we do not specifically enumerate the requirements, but yes, we recommend the entrainment formulation when all are fulfilled. See Lines 618-634 of the manuscript with track changes.

39. Ln 643-646. Please provide some more information here. When more information is added this

finding should be one of the main results, I think. Also see suggestion on research questions.

We have expanded this in the new text. See Lines 726-732 of the manuscript with track changes.

40. Line 681. Please explain why the time derivatives may be omitted.

In principle, the time derivatives cannot be omitted. But for the purpose of illustrating the spatial lag, the analysis is clear if we omit the time derivatives. By the same token, in order to illustrate temporal lag, it is clearer to omit the spatial derivatives.

41. Ln 17 and 45. alternate → alternative?

The manuscript has been revised as suggested by the reviewer.

42. Ln 35. Reference to Parker 2004 can be omitted.

Reference to Parker 2004 has been deleted here.

43. Ln 85. bed material → surface or substrate?

The data in Figure 1(c) is based on the sampling of the bed surface. We have modified the text to clarify this. See Line 91 of the manuscript with track changes.

44. Ln 90. "and thus more likely to be" → "as it is".

The manuscript has been revised as suggested by the reviewer.

45. Ln 141. I think the 0.4 value should be listed at a later point in the manuscript.

The 0.4 value has been moved to Section 3. See Line 305 of the manuscript with track changes.

46. Ln 154. "La is often related to the height of dunes so that" → "La is often related to the height of dunes (Blom, 2008) so that".

The manuscript has been revised as suggested by the reviewer.

47. Ln 161 and 162. You'll need to apply Eq (6) to n-1 sediment fractions.

The reviewer is right that Eq (6) is applied to n-1 sediment fractions in the model. Here we only show the general formulation of the equation system.

48. Ln 248-249. I'd rephrase 'hiding effects between coarse and fine sediment'.

The manuscript has been rewritten to explain the way that equations (24)-(27) work. See Lines

267-273 of the manuscript with track changes.

49. Ln 267. Blom et al 2003 → Blom 2008.

The reference has been changed as suggested by the reviewer.

50. Ln 277 and 621. I'd avoid using "=" like this in a sentence.

The "=" has been removed.

51. Ln 283 and 284. I'd change the unit years to something much smaller.

We would like to keep the unit years partly because the concept of flood intermittency factor is basically considered in the time scale of years.

52. Ln 285-287. I'd rephrase the following sentence: "But it should be noted that the aim of this paper is not to reproduce specific aspects of the morphodynamic processes of LYR, but to compare the flux form and entrainment form of Exner equation in the context of conditions typical of LYR."

We are not sure how to rephrase. The sentence correctly highlights the goals of the paper.

53. Fig 2. Caption and legend. "Initial bed" refers to surface or substrate? "Washload sizes" refers to which sizes?

"Initial bed" refers to both the initial surface and initial substrate. "Washload sizes" refer to grain sizes which belongs to the range of washload, i.e. < 15 μm.

54. Ln 436-437. Why repeat an equation?

We repeat for clarity. We do not want the reader to have to look many pages back to understand our argument.

55. Ln 621. I'd avoid starting a sentence with "But".

OK, changed.

56. Ln 617 Sentence starting with "Moreover, …unchanged". I'd omit this.

Three fairly large chunks of text related to arbitrarily increased or decreased fall velocity have been deleted from the Conclusion. See Lines 700-702, Lines 708-709, and Lines 714-718 of the manuscript with track changes.

Reviewer #2

1. My major concern is the generality of the results given the effect of the upstream boundary on model results in all cases where the upstream sediment input is less than capacity. In these cases, there is degradation at the upstream boundary and a gradual, exponential, rise towards capacity transport at some distance downstream. Such a situation is appropriate immediately below a dam, but without such a barrier to sediment transport the transport rate (sediment input) at the boundary would be in equilibrium with local flow conditions and availability of sediment on the river bed.

Morphodynamics is the essence of response to disequilibrium conditions inducing aggradation, degradation and sorting. Cutoff of sediment supply due to a dam is both an excellent way to study response to disequilibrium and characterize a key factor presently affecting the LYR.

In our simulations, we implement sediment supply rates which are less than sediment transport capacity. Such a situation is appropriate for the LYR or other alluvial rivers which are affected by dams. However, we think that the general conclusions of this paper are also applicable to other kind of perturbations which lead to an imbalance between the sediment supply and sediment transport capacity. Bed aggradation or degradation would occur from the place where perturbation is introduced, and sediment concentration (or sediment transport rate) would adjust exponentially to its equilibrium value.

As for the situation under which the sediment supply equals sediment transport capacity as suggested by the reviewer, we think that this situation does not shed light on our problem, because there would be no bed evolution, i.e. nothing would happen.

2. Much of the paper addresses the conditions under which the model predicts diffusion and/or advection. The analysis of this aspect is very useful and provides a way of evaluating how perturbations should be translated downstream. There is no consideration of the extent to which the model behavior may reflect numerical behavior. Morphological models of this type tend to be diffusive, for reasons that are considered in the paper and which relate to the damping effect as the bed surface (gradient and grain size) co-evolve in response to divergence in the sediment transport rate. Advection is not surprising where significant disturbances are introduced, especially where transport rates are relatively high. However, I find it difficult to understand how the model can generate successive advective waves (lines 627-35 are convincing, but for one wave), and wonder if there are aspects to the behaviour of the sediment transport function and/or sediment routing that lead to this. For example, it is unclear if the active layer thickness is maintained (ie is the surface layer mixed with the sub-surface at every timestep, or is the active layer exhausted and then replenished from the subsurface only after this exhaustion is complete? This latter approach could readily lead to generation of additional waves of adjustment as the sub-surface will be finer than the surface in the surface layer).

The issue of successive advective waves has been discussed thoroughly in Stecca et al. (2014, 2016). The number of kinematic waves actually depend on the discretization of the grain size distribution: each grain size fraction would induce the migration of one wave. We have explained this in the manuscript. See Lines 418-419 of the manuscript with track changes. The reviewer may also refer to Stecca et al. (2014, 2016) for more information.

When solving Equation (6) or Equation (15), the active layer exchange with the sediment suspended load as well as the substrate at the same time in every time step.

3. Lines 248-9: following the previous comment, it would be useful to know a little more about the way that equations (24)-(27) work. Did Ma et al (2017) use a size-specific formulation too?

The manuscript has been rewritten to explain the way that equations (24)-(27) work. See Lines 267-273 of the manuscript with track changes. Ma et al. (2017) did not use a size-specific formulation. Their relation calculates the total sediment transport rate with a characteristic grain size.

4. Lines 88-90: I am unclear that the entrainment-based approach is more physically based than the flux-based approach. A properly-calibrated transport model should work just as well for the flux-based approach – if this predicts transport rates that exceed observations, this suggests to me a problem with the transport equation rather than needing a 'supply-limitation' correction factor applying. I also do not see the relevance of saying that Chinese researchers have a particular approach.

We think that the entrainment-based approach is more physically based than the flux-based approach, because the entrainment-based approach considers lag effects (nonequilibrium sediment transport) whereas the flux-based approach cannot. The difference between the two approaches becomes more evident for finer sediment. We show that the difference is physically based. Solving the problem through calibration is not as satisfying as solving it through physics. We do indeed think that it is relevant to mention the Chinese LYR modeling approach heretofore, because we wish to influence this audience, as well as the general morphodynamics community.

5. Line 92: is the additional computational requirement significant – I suspect not.

According to our experience, the additional computational requirement is significant. The main reason is that the governing equations for sediment concentration need to be solved in the entrainment-based approach but do not need to be solved in the flux-based approach. For a sediment GSD with n size ranges, n more equations need to be solved every time step. Moreover, when dealing with fine sediment, a small time step is be needed to solve the additional governing equations of sediment concentration.

6. Lines 117-8 (and others): using a simplified geometry is entirely justified and makes a lot of sense. However, some consideration of the potential significance of these assumptions would be useful. For example, downstream of the dam is degradation uniform across the channel or is it concentrated in a thalweg leading to asymmetric cross-section geometry? On lines 253-4, can some indication be given about the observed variation in width and slope? I assume that there are no significant tributary inflows of water and/or sediment, and this could be stated here too.

Some explanation has been added to the manuscript as suggested by the reviewer. See Lines 127-137, and Lines 666-673 of the manuscript with track changes.

7. Following the previous comment, it would be good to have some more assessment of model

performance. Some annual flux estimate comparisons are made, which are encouraging. Are there other pieces of evidence (eg order of magnitude of degradation below the dam, and distance of propagation of the degradational wave after some years) that can be used to provide a general validation of the model?

Our model overpredicts degradation. There are two reasons for this. 1) We have assumed that the sediment supply to the LYR is 10% of the pre-Xiaolangdi value. The actual number is closer to 20%. We chose the lower number in order to clearly see the difference between the two (flux and entrainment) models. In addition, our sediment transport relation does not undergo a phase change to lower sediment transport regime as the bed coarsens beyond 100 μm. We are working on a new sediment transport relation which includes this phase change. The issue is important, but not relevant to the major point of this paper, i.e. flux versus entrainment.

8. Line 156 (and others): given the seasonal flow regime of this river, there will be variation in dune height during the sediment transporting period. I appreciate the use of constant flow and La for these simulations, but could the effect of La changing in time be considered?

In this paper we relate the active layer thickness to the height of bedforms, which is 20% of the flow depth for the LYR according to Ma et al. (2017). A constant active layer thickness is implemented based on the equilibrium flow depth before the cutoff of sediment supply.

We agree with the reviewer that the dune height might change during the sediment transport period. But since the adjustment of bedforms is mostly much slower than the adjustment of flow hydraulics (i.e., the morphodynamic timescale is much larger than the hydraulic timescale), relating the active layer thickness directly to the instantaneous flow depth might be incorrect. Therefore, the assumption of constant active layer thickness can be regarded as an average for long-term hydraulic conditions. The question of how to quantify the instantaneous active layer thickness merits future study.

9. Model comparison (Line 364) – using absolute values is actually less informative than retaining the signs (or using yE/yF ratios). Table 2 (and later tables) – I did not find these tables very helpful, and wonder if it would be better to put this information onto the relevant figures as an additional plot (Lines 414-422 are very wordy as a result of describing Table 3 – would be easier to describe a graph of the same results). The figures on the table definitely do not need to be 2 decimal places.

We have kept the tables but changed the numbers to one digit after the decimal point.

10. Line 344: ‘intentionally unrealistic’ is ok, but readers might assume linear behavior between your realistic and unrealistic boundary conditions. Do you know if this is a reasonable assumption to make?

The parameter in question is fall velocity, which is not a boundary condition. While not linear, adaptation length monotonically increases with decreasing fall velocity.

11. Lines 451-2: I think (from memory – don’t have the paper to hand) that this is similar to Philipps

and Sutherland's formulation. If so, maybe reference this here.

The formulation of Phillips and Sutherland (1989) deals with bedload, not suspended load.

12. Lines 467-8: another way to interpret this is in terms of settling velocity (ie there is a settling velocity, or Stokes number, above which adaptation length can be ignored).

We agree with the reviewer that the adaptation can also be analyzed via settling velocity. But since settling velocity is a function of grain size, we think that it does not make much difference whether using settling velocity or grain size as the independent variable. Actually equation (31) (which is also exhibited in Figure 9) shows how adaptation length is controlled by the settling velocity.

13. Lines 555-7: I am not sure that the results in this paper can be used to make recommendations about event-scale modelling. It would be good to see some event-scale simulations to assess the significance of any differences between the two formulations.

Additional numerical cases with hydrographs have been added in the Supplement. Results indicate that our conclusions based on constant flow discharge also hold when hydrographs are implemented. See Sections S2 and S3 of the Supplement.

We have also moved Appendix A and Appendix B to the Supplement.

14. Line 28: I would say 'adapted for' rather than 'designed for'.

The manuscript has been revised as suggested by the reviewer.

15. Line 36: 'some aspect of sediment transport' is rather imprecise – can this be made more specific.

The manuscript has been rewritten to make the description more specific. The "aspect" is sediment transport itself. See Line 39 of the manuscript with track changes.

16. Line 119: presumably the grain-size distribution of the flux is also fixed?

Yes. Sediment of each grain size range is fed at a specific rate, which means the grain size distribution of the sediment supply is also fixed. The manuscript has been revised to make this issue clear. See Line 133 of the manuscript with track changes.

17. Lines 271-2: can the sorting of the gsd also be given (maybe use the blank spaces on Figure 2 to put these numbers onto)?

We have added the geometric standard deviation. See Lines 300-301 of the manuscript with track changes.

18. Line 281: I think it is 400 cells, but 401 computational nodes.

Since the finite volume method is implemented for the hydraulic calculation, our numerical method is based on cells rather than nodes. The channel length is 200 km, and the cell size is 0.5 km. Actually we have 401 cells with cell centers located at x = 0 km, 0.5 km, 1 km, … , 199 km, 199.5 km, and 200 km.

19. Line 282: can you give Courant numbers for these timesteps?

The Courant number is defined as (u+(g*h)^0.5)*dth/dx, where u is flow velocity, h is flow depth, and dth is the time step for hydraulic calculation. The Courant number in all cases of our simulations is no more than 0.1.

20. Table 1: Add dx and dt to this – the table is a very useful quick reference point, so having these values here would be informative.

The values of dx and dt have been added to Table 1.

21. Figure 3: Could the water surface be added to this plot (maybe initial and final values only)?

Initial and final water surfaces have been added to Figures 3-8.

References:

Armanini, A. and Di Silvio, G.: A one-dimensional model for the transport of a sediment mixture in non-equilibrium conditions, Journal of Hydraulic Research, 26(3), 275-292, doi:10.1080/00221688809499212, 1988.

Bell, R. G. and Sutherland, A. J.: Nonequilibrium bedload transport by steady flows, Journal of Hydraulic Engineering, 109(3), 351-367, 1983.

El kadi Abderrezzak, K. and Paquier, A.: One-dimensional numerical modeling of sediment transport and bed deformation in open channels, Water Resources Research, 45, W05404, doi:10.1029/2008WR007134, 2009.

Ma, H., Nittrouer, J. A., Naito, K., Fu, X., Zhang, Y., Moodie A. J., Wang, Y., Wu, B., and Parker, G.: The exceptional sediment load of fine-grained dispersal systems: Example of the Yellow River, China, Science Advances, 3(5), e1603114, doi:10.1126/sciadv.1603114, 2017.

Pelosi, A. and Parker, G.: Morphodynamics of river bed variation with variable bedload step length, Earth Surface Dynamics, 2, 243-253, doi:10.5194/esurf-2-243-2014, 2014.

Phillips, B. C. and Sutherland A. J.: Spatial lag effects in bedload sediment transport, Journal of Hydraulic Research, 27(1), 115-133, doi:10.1080/00221688909499247, 1989.

Stecca, G., Siviglia, A., and Blom, A.: Mathematical analysis of the Saint-Venant-Hirano model for mixed-sediment morphodynamics, Water Resources Research, 50, 7563–7589, doi:10.1002/2014WR015251, 2014.

Stecca, G., Siviglia, A., and Blom, A.: An accurate numerical solution to the Saint-Venant-Hirano model for mixed-sediment morphodynamics in rivers, Advances in Water Resources, 93(Part A), 39-61, doi:10.1016/j.advwatres.2015.05.022, 2016.

Morphodynamic model of Lower Yellow River: flux or entrainment form for sediment mass conservation?

Chenge An[1], Andrew J. Moodie[2], Hongbo Ma[2], Xudong Fu[1], Yuanfeng Zhang[3], Kensuke Naito[4], Gary Parker[5]

[1]Department of Hydraulic Engineering, State Key Laboratory of Hydroscience and Engineering, Tsinghua University, Beijing, China.
[2]Department of Earth, Environmental and Planetary Sciences, Rice University, Houston, TX, USA.
[3]Yellow River Institute of Hydraulic Research, Zhengzhou, Henan, China.
[4]Department of Civil and Environmental Engineering, Hydrosystems Laboratory, University of Illinois, Urbana-Champaign, IL, USA.
[5]Department of Civil and Environmental Engineering and Department of Geology, Hydrosystems Laboratory, University of Illinois, Urbana-Champaign, IL, USA.

Correspondence to: Chenge An (anchenge08@163.com) and Xudong Fu (xdfu@tsinghua.edu.cn)

Abstract. Sediment mass conservation is a key factor that constrains river morphodynamic processes. In most models of river morphodynamics, sediment mass conservation is described by the Exner equation, which may take various forms depending on the problem in question. One of the most widely used forms of the Exner equation is the flux-based formulation, in which the conservation of bed material is related to the streamwise gradient of the sediment transport rate. An ~~alternate~~ alternative form of the Exner equation, however, is the entrainment-based formulation, in which the conservation of bed material is related to the difference between the entrainment rate of bed sediment into suspension and the deposition rate of suspended sediment onto the bed. In the flux form, sediment transport ~~is regarded to be in local equilibrium (i.e., sediment transport rate~~ is a local function of bed shear stress~~locally equals sediment transport capacity)~~. However, the entrainment form does not require this constraint: only the rate of entrainment into suspension is in local equilibrium, and the sediment transport rate itself may lag in space and time behind the changing flow conditions. Here we identify the flux form as based on the local capacity sediment transport rate, and the entrainment form as based on the local capacity entrainment rate. In modeling the fine-grained Lower Yellow River, it is usual to treat sediment conservation in terms of an entrainment (nonequilibrium) form rather than a flux (equilibrium) form, in consideration of the condition that fine-grained sediment may be entrained at one place but deposit~~ed~~ only at some distant location downstream. However, the differences in prediction between the two formulations have not been comprehensively studied to date. Here we study this problem by comparing the results predicted by both the~~of~~ flux ~~based~~ form and the entrainment ~~based~~ form of the Exner equation, ~~morphodynamics~~ under conditions simplified from ~~typical of~~ the Lower Yellow River (i.e. a significant reduction of sediment supply after the closure~~operation~~ of the Xiaolangdi Dam)~~, but simplified for clarity of comparison~~. We use~~d~~ sediment transport equations specifically ~~designed~~ adapted for the Lower Yellow River. We find that in a treatment of a 200 km reach using a single characteristic bed sediment size, there is little difference between the two forms since the corresponding adaptation length is relatively small. However, a consideration of sediment mixtures

shows that the two forms give very different patterns of grain sorting: clear kinematic waves occur in the flux form but are diffused out in the entrainment form. Both numerical simulation and mathematical analysis show that the morphodynamic processes predicted by the entrainment form are sensitive to sediment fall velocity.

1. Introduction

Models of river morphodynamics often consist of three elements ~~(Parker, 2004)~~: (1) a treatment of flow hydraulics; (2) a formulation relating ~~some aspect of~~ sediment transport ~~(e.g. volumetric sediment transport rate)~~ to flow hydraulics; and (3) a description of sediment conservation. In the case of unidirectional river flow, the Exner equation of sediment conservation has usually been described in terms of a flux-based form in which temporal bed elevation change is related to the streamwise gradient of the sediment transport rate. That is, bed elevation change is related to $\partial q_s/\partial x$, where q_s is the total volumetric sediment transport rate per unit width and x is the streamwise coordinate (Exner, 1920; Parker et al., 2004). This formulation is also referred to as the equilibrium formulation, since it considers sediment transport to be at local equilibrium, i.e. q_s equals its sediment transport capacity q_{se}, as defined by the sediment transport rate associated with local bed shear stress, regardless of the variation of flow conditions. Under this assumption, sediment transport relations developed under equilibrium flow conditions (e.g., Meyer-Peter and Müller, 1948; Engelund and Hansen, 1967; Brownlie, 1981) can be incorporated directly in such a formulation to calculate q_s, which is related to one or more flow parameters such as bed shear stress.

An alternate formulation, however, is available in terms of an entrainment-based form of the Exner equation, in which bed elevation variation is related to the difference between the entrainment rate of bed sediment into ~~suspension~~ the flow~~water~~ and the deposition rate of ~~suspended~~ sediment on the bed (Parker, 2004). The basic idea of the entrainment formulation can be traced back to Einstein's (1937)~~'s~~ pioneering work of bedload transport, and has been developed since then by numerous researchers so as to treat either bedload or suspended load (Tsujimoto, 1978; Armanini and Di Silvio, 1988; Parker et al., 2000; Wu and Wang, 2008; Guan et al., 2015). Such a formulation differs from the flux formulation in that it is the rate of entrainment of bed sediment, rather than the sediment transport rate itself, that is related to flow hydraulics. The difference between the local entrainment rate from the bed and the local deposition rate onto the bed determines the rate of bed aggradation/degradation, and concomitantly the rate of loss/gain of sediment in motion in the water column. Therefore, the sediment transport rate is no longer assumed to be in an equilibrium transport state, but may exhibit lags in space and time after changing flow conditions. The entrainment formulation is also referred to as the nonequilibrium formulation (Armanini and Di Silvio, 1988; Wu and Wang, 2008; Zhang et al., 2013).

To describe the lag effects between sediment transport and flow conditions, the concept of an adaptation length/time is widely applied. This length/time characterizes the distance/time for sediment transport to reach its equilibrium state (i.e., transport capacity). Using the concept of the adaptation length, the Exner equation can be recast into a first-order "reaction" equation, in which the deformation term is related to the difference between the actual and equilibrium sediment transport rates, as mediated by an adaptation length (which can also be recast as an adaptation time). (Armanini and Di Silvio, 1988;

Wu and Wang, 2008; Minh Duc and Rodi, 2008; El kadi Abderrezzak and Paquier, 2009). The adaptation length is thus an important parameter for bed evolution under nonequilibrium sediment transport conditions, and various estimates have been proposed. For suspended load, the adaptation length is typically calculated as a function of flow depth, flow velocity and sediment fall velocity (Armanini and Di Silvio, 1988; Wu et al., 2004; Wu and Wang, 2008; Dorrell and Hogg, 2012; Zhang et al., 2013). The adaptation length of bedload, on the other hand, has been related to a wide range of parameters, including the sediment grain size (Armanini and Di Silvio, 1988), the saltation step length (Phillips and Sutherland, 1989), the dimensions of particle diffusivity (Bohorquez and Ancey, 2016), the length of dunes (Wu et al., 2004), and the magnitude of a scour hole formed downstream of an inerodible reach (Bell and Sutherland, 1983). For simplicity, the adaptation length can also be specified as a calibration parameter in river morphodynamic models (El kadi Abderrezzak and Paquier, 2009; Zhang and Duan, 2011). Nonetheless, no comprehensive definition of adaptation length exists.

In this paper we apply the two forms of the Exner equation mentioned above to the Lower Yellow River (LYR) in China. The LYR describes the river section between Tiexie and the river mouth, and has a total length of about 800 km. Figure 1(a) shows a sketch of the LYR along with 6 major gauging stations and the Xiaolangdi Dam, which is 26 km upstream of Tiexie. The LYR has an exceptionally high sediment concentration (Ma et al., 2017), historically exporting more than 1 Gt of sediment per year with only 49 billion tons of water, leading to a sediment concentration an order of magnitude higher than most other large lowland rivers worldwide (Milliman and Meade, 1983; Ma et al., 2017; Naito et al., accepted subject to revision). However, the LYR has seen a substantial reduction in its sediment load in ~~the~~ recent decades, especially ~~More recently, however,~~ since the operation of Xiaolangdi Dam in 1999 ~~the LYR has seen a substantial reduction in its sediment load~~ (Fig. 1(b)), because most of ~~the~~ its sediment load is derived from the Loess Plateau which is ~~river reach~~ upstream of the reservoir~~, especially from the Loess Plateau~~ (Wang et al., 2016; Naito et al., accepted subject to revision). Finally, the bed surface material of the LYR is very fine, ranging as low as 15 μm. This is much finer than the conventional cutoff of washload (62.5 μm) employed for sediment transport in most sand-bed rivers (National Research Council, 2007; Ma et al., 2017).

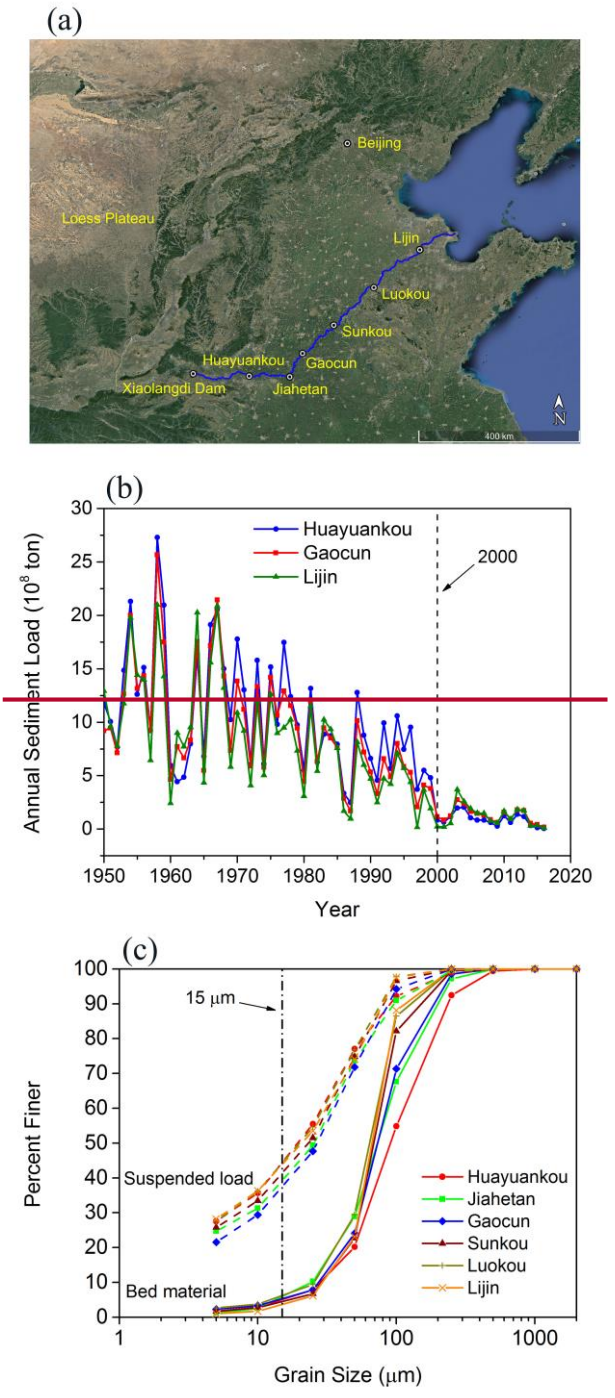
(a)
Beijing
Loess Plateau
Lijin
Luokou
Sunkou
Huayuankou
Gaocun
Xiaolangdi Dam
Jiahetan
N
400 km
(b)
Huayuankou
Gaocun
Lijin
2000
Annual Sediment Load (10^8 ton)
Year
(c)
15 μm
Suspended load
Bed material
Huayuankou
Jiahetan
Gaocun
Sunkou
Luokou
Lijin
Percent Finer
Grain Size (μm)

88

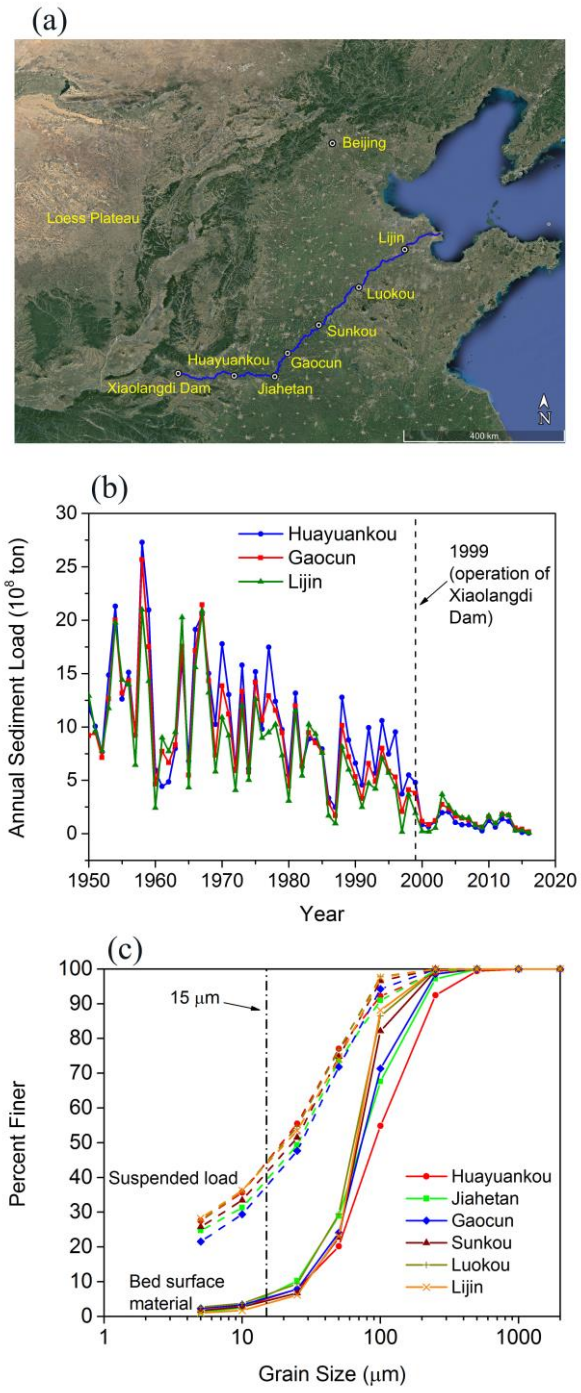

Figure 1. (a) Sketch of Lower Yellow River, showing 6 major gauging stations and the Xiaolangdi Dam; (b) Annual sediment load of LYR measured at 3 gauging stations since 1950; (c) Grain size distributions of both bed surface material and suspended load measured at 6 gauging stations of the LYR.

When modeling the high-concentration and fine-grained LYR, it is common to treat sediment conservation in terms of an entrainment-based rather than a flux-based formulation. This is because many Chinese researchers view the entrainment formulation as more physically based, ~~and thus more likely to be~~as it is capable of describing the behavior of fine-grained sediment, which when entrained at one place may be deposited at some distant location downstream (Zhang et al., 2001; Ni et al., 2004; Cao et al., 2006; He et al., 2012; Guo et al., 2008). However, the entrainment formulation is more computationally expensive and more complex to implement. In so far as the differences in prediction between the two formulations do not appear to have been studied in a systematic way, here we pose our central questions. ~~Is the entrainment formulation really necessary when modeling the LYR?~~Under what conditions is it valid to use the entrainment form of the Exner equation, and under what conditions may the flux form be used?~~Under what conditions should one apply an entrainment form or flux form description of the Exner equation?~~ Or more specifically, which form of the Exner equation is most suitable for the LYR?~~under what circumstances should a numerical modeler be impelled to implement the entrainment formulation instead of the flux formulation for river morphodynamic modeling?~~

Here we study this problem by comparing the results of flux-based and entrainment-based morphodynamics under conditions typical of the LYR. The organization of this paper is as follows. The numerical model is described in Section 2. In Section 3, the model is implemented to predict the morphodynamics of the LYR with a sudden reduction of sediment supply, which servesis to mimic the effect of Xiaolangdi Dam. We find that the two forms of the Exner equation give similar predictions in the case of uniform sediment, but show different sorting patterns in the case of sediment mixtures. In Section 4, we conduct a mathematical analysis to explain the results in Section 3, and more specifically we quantify the effects of varied sediment fall velocity in the simulations. Finally, we summarize our conclusions in Section 5.

2. Model formulation

In this paper, we present a one-dimensional morphodynamic model for the Lower Yellow River. The fully unsteady Saint Venant Equations are implemented for the hydraulic calculation. ~~As the main topic of this paper is to compare the flux form and entrainment form of Exner equation, b~~Both the flux form and the entrainment form ~~formulations~~ of the Exner equation are implemented in the model for sediment mass conservation~~ are implemented~~. For each ~~formulation~~form of Exner equation, we consider both the cases of uniform sediment (bed material characterized by a single grain size) and sediment mixtures. Since the sediment is very fine in the LYR, the component of the load that is bedload is likely negligible (e.g. Ma et al., 2017), so that we consider only the transport of suspended load. Considering the fact that most ~~well~~ accepted sediment transport relations (e.g., the Engelund and Hansen. 1967 relation) underpredict the sediment transport rate of the LYR by an order of magnitude or more (Ma et al., 2017), in our model we implement two recently developed generalized versions of the Engelund-Hansen relation which are based on data from the LYR. These are the version of Ma et al. (2017) for uniform sediment, and the version of Naito et al. (accepted subject to revision) for sediment mixtures. In cases considering sediment

mixtures, we also implement the method of Viparelli et al. (2010) to store and access bed stratigraphy as the bed aggrades and degrades.

Since the aim of this paper is to compare the two formulations of the Exner equation in context of the LYR, rather than reproduce ~~the~~ site-specific morphodynamic processes of the LYR, ~~S~~some additional simplifications are introduced to the model to facilitate ~~comparison across the Exner formulation model runs~~comparison. The channel is simplified to be a constant-width rectangular channel, and bank (sidewall) effects and floodplain interactions are not considered. The channel bed is assumed to be an infinitely deep supplier of erodible sediment with no exposed bedrock, which is justifiable because ~~since~~ the LYR is fully alluvial, and has been aggrading for thousands of years, as copiously documented in Chinese history. Finally, water and sediment (of each grain size range) are fed into the upstream boundary at a specified rate, and at the downstream end of the channel we specify a fixed bed elevation along with a normal flow depth. These restrictions could be easily relaxed so as to incorporate site-specific complexities of the Yellow River. Because of the severe aggradation of the LYR developed before the Xiaolangdi Dam operation, the LYR is famous for its hanging bed (i.e. bed elevated well above the floodplain) and no major tributaries need ~~to~~ be considered in the simulation.

2.1 Flow hydraulics

Flow hydraulics in a rectangular channel is described by the following 1D Saint Venant equations, which consider ~~the~~ fluid mass and momentum conservation,

$$\frac{1}{I_f}\frac{\partial h}{\partial t}+\frac{\partial q_w}{\partial x}=0 \tag{1}$$

$$\frac{1}{I_f}\frac{\partial q_w}{\partial t}+\frac{\partial}{\partial x}\left(\frac{{q_w}^2}{h}+\frac{1}{2}gh^2\right)=ghS-C_f u^2 \tag{2}$$

$$C_f = C_z^{-2} \tag{3}$$

where t is time, h is water depth, q_w is flow discharge per unit width, g is gravitational acceleration, S is bed slope, u is depth-averaged flow velocity, C_f is dimensionless bed resistance coefficient, and C_z is the dimensionless Chezy resistance coefficient. In our model, the fully unsteady 1D Saint Venant equations are solved using a Godunov type scheme with the HLL (Harten-Lax-van Leer) approximate Riemann solver (Harten et al., 1983; Toro, 2001), which can effectively capture discontinuities in unsteady and nonuniform open channel flows.

In this paper, the full flood hydrograph of the LYR is replaced by a flood intermittency factor I_f (Paola et al., 1992; Parker, 2004). According to this definition, the river is assumed to be at low flow and not transporting significant amounts of sediment for time fraction 1 - I_f; and is in flood at constant discharge and active morphodynamically for time fraction I_f. In the

long term, the relation between the flood time scale t_f and the actual time scale t is $t_f = I_f t$. For all the governing equations in this paper, the flood time scale is implemented by introducing I_f into each time derivative. Full hydrographs are considered in the Supplement.

2.2 Flux form of the Exner equation

When dealing with uniform sediment, the flux form of the Enxer equation can be written as,

$$\frac{1}{I_f}\left(1-\lambda_p\right)\frac{\partial z_b}{\partial t} = -\frac{\partial q_s}{\partial x} \tag{4}$$

where λ_p is the porosity of the bed deposit, ~~taken to be 0.4 in this paper~~ and z_b is bed elevation. Sediment transport is regarded to be in a quasi-equilibrium state, so that the sediment transport rate per unit width q_s equals the equilibrium (capacity) sediment transport rate per unit width q_{se}.

When considering sediment mixtures, an active layer formulation (Hirano, 1971; Parker, 2004) is incorporated in the flux-based Exner equation, so that the evolution of both bed elevation and surface grain size distribution can be considered. In this formulation, the river bed is divided into a well-mixed upper active layer and a lower substrate with vertical stratigraphic variations. The upper active layer therefore represents the volume of sediment that interacts directly with suspended load transport, and also exchanges with the substrate as the bed aggrades and degrades. Discretizing the grain size distribution into n ranges, the mass conservation relation for each grain size range can be written as,

$$\frac{1}{I_f}\left(1-\lambda_p\right)\left[f_{Ii}\frac{\partial}{\partial t}\left(z_b - L_a\right) + \frac{\partial}{\partial t}\left(F_i L_a\right)\right] = -\frac{\partial q_{si}}{\partial x} \tag{5}$$

where q_{si} is volumetric sediment transport rate per unit width of the i-th grain size range (taken to be equal to its equilibrium value q_{sei} in the flux formulation), F_i is the volumetric fraction of surface material in the i-th grain size range; f_{Ii} is volumetric fraction of material in the i-th grain size range exchanged across the surface-substrate interface as the bed aggrades or degrades, and L_a is the thickness of active layer. For bedform-dominated sand-bed rivers, L_a is often related to the height of dunes (Blom, 2008) so that the vertical sorting processes due to bedform migration can be considered ~~(Blom et al., 2003)~~. In this paper, a constant value of L_a is implemented in the simulation.

Summing Eq. (5) over all grain size ranges, one can find that the governing equation for bed elevation in case of sediment mixtures is the same as Eq. (4) upon replacing q_s with $q_{sT} = \Sigma q_{si}$, where q_{sT} denotes the total sediment transport rate per unit width summer over all size ranges. Reducing Eq. (5) with Eq. (4) we get,

$$\frac{1}{I_f}\left(1-\lambda_p\right)\left[L_a\frac{\partial F_i}{\partial t} + \left(F_i - f_{Ii}\right)\frac{\partial L_a}{\partial t}\right] = f_{Ii}\frac{\partial q_{sT}}{\partial x} - \frac{\partial q_{si}}{\partial x} \tag{6}$$

Therefore, in the flux formulation Eqs. (4) and (6) are implemented as governing equations for sediment mixtures, with Eq. (4) describing the evolution of bed elevation and Eq. (6) describing the evolution of surface grain size distribution. The exchange fractions f_{Ii} between the active layer and the substrate are calculated using the following closure relation,

$$f_{Ii} = \begin{cases} f_i\,|_{z_b - L_a} & \dfrac{\partial\left(z_b - L_a\right)}{\partial t} < 0 \\ \alpha F_i + \left(1-\alpha\right) p_{si} & \dfrac{\partial\left(z_b - L_a\right)}{\partial t} > 0 \end{cases} \tag{7}$$

That is, the substrate is transferred into the active layer during degradation, and a mixture of suspended load and active layer material is transferred into substrate during aggradation. In Eq. (7), $f_i|_{zb\text{-}La}$ is the volumetric fraction of substrate material just beneath the interface, $p_{si} = q_{si}/q_{sT}$ is the fraction of bed material load in the i-th grain size range, and α is a specified parameter between 0 and 1 The formulation is adapted from Hoey and Ferguson (1994) and Toro-Escobar et al. (1996), who originally used it for bedload. In this paper, a value of 0.5 is specified for α.

The method of Viparelli et al. (2010) is applied in our model to store substrate stratigraphy and provide information for $f_i|_{zb\text{-}La}$ (i.e., the topmost sublayer in Viparelli et al., 2010). The reader can refer to the original reference of Viparelli et al. (2010) for more details, or refer to An et al. (2017) for a concise description as to how to implement this method in a morphodynamic model.

2.3 Entrainment form of the Exner equation

The entrainment-based Exner equation for uniform sediment is,

$$\frac{1}{I_f}\left(1-\lambda_p\right)\frac{\partial z_b}{\partial t} = -v_s\left(E - r_0 C\right) \tag{8}$$

In Eq. (8), v_s is the fall velocity of sediment particles; E is the dimensionless entrainment rate of sediment normalized by sediment fall velocity; C is the depth-flux-averaged volume sediment concentration; and $r_o = c_b/C$ is the recovery coefficient of suspended load which denotes the ratio between the near-bed sediment concentration c_b and the flux-averaged sediment concentration C. By definition, r_0 is related to the concentration profile of suspended load, and is expected to be no less than unity in cases appropriate for a depth-averaged shallow-water treatment of flow and morphodynamics.

For the sediment fall velocity v_s, we compare two widely used relations: the relation of Dietrich (1982), and the relation of Ferguson and Church (2004). Results show that these two relations give almost the same fall velocity for bed material load of the LYR, whose grain sizes typically fall in the range of 15 μm to 500 μm. Therefore, only the relation of Dietrich (1982) is implemented in our simulations in this paper. Readers can refer to ~~Appendix A~~Section S1 of the Supplement ~~Information~~ for more details.

Since sediment transport is not necessarily in its equilibrium state in the entrainment formulation, we back-calculate~~relate~~ the sediment entrainment rate from~~, rather than the sediment transport rate, to~~ the equilibrium sediment transport rate. Thus

$$E = r_0 \frac{q_{se}}{q_w} \tag{9}$$

For the depth-flux-averaged sediment concentration C, another equation is implemented describing the conservation of suspended sediment in the water column,

$$\frac{1}{I_f}\frac{\partial(hC)}{\partial t} + \frac{\partial(huC)}{\partial x} = v_s\left(E - r_0 C\right) \tag{10}$$

Note that sediment transport is at equilibrium when $E = r_o C$. The sediment transport rate per unit width q_s obeys a continuity relation,

$$q_s = huC \tag{11}$$

The entrainment-form Exner equation for sediment mixtures also uses the active layer formulation described in Section 2.2. Mass conservation of each grain size range can be written as,

$$\frac{1}{I_f}\left(1-\lambda_p\right)\left[f_{Ii}\frac{\partial}{\partial t}\left(z_b - L_a\right) + \frac{\partial}{\partial t}\left(F_i L_a\right)\right] = -v_{si}\left(E_i - r_{0i}C_i\right) \tag{12}$$

$$E_i = r_{0i}\frac{q_{sei}}{q_w} \tag{13}$$

where the subscript i denotes the i-th size range of sediment grain size.

Summing Eq. (12) over all grain size ranges, we get the governing equation for bed elevation,

$$\frac{1}{I_f}\left(1-\lambda_p\right)\frac{\partial z_b}{\partial t} = -\sum_{j=1}^{n} v_{sj}\left(E_j - r_{0j}C_j\right) \tag{14}$$

Reducing Eq. (12) with Eq. (14) we get the governing equation for surface fraction F_i,

$$\frac{1}{I_f}\left(1-\lambda_p\right)\left[L_a\frac{\partial F_i}{\partial t} + \left(F_i - f_{Ii}\right)\frac{\partial L_a}{\partial t}\right] = f_{Ii}\sum_{j=1}^{n} v_{sj}\left(E_j - r_{0j}C_j\right) - v_{si}\left(E_i - r_{0i}C_i\right) \tag{15}$$

The governing equation for the sediment concentration of each grain size C_i can be written as,

$$\frac{1}{I_f}\frac{\partial\left(hC_i\right)}{\partial t}+\frac{\partial\left(huC_i\right)}{\partial x}=v_{si}\left(E_i-r_0C_i\right) \tag{16}$$

and the sediment transport rate per unit width for the *i*-th size range q_{si} obeys the following continuity relation,

$$q_{si}=huC_i \tag{17}$$

In the entrainment formulation, the closure relation for f_{li} is the same as that used in the flux formulation (i.e., Eq. (7)), and the substrate stratigraphy is also stored and accessed using the method of Viparelli et al. (2010).

2.4 Sediment transport relation

2.4.1 Uniform sediment

To close the Exner equations described in Sections 2.2 and 2.3, equations for equilibrium sediment transport rate q_{se} (q_{sei}) are still needed. For the simulations using uniform sediment, we implement the generalized Engelund-Hansen relation proposed by Ma et al. (2017). This equation is based on the data from LYR and can be written in the following dimensionless form,

$$q_s^*=\frac{\alpha_s}{C_f}\left(\tau^*\right)^{n_s} \tag{18}$$

where q_s^* is dimensionless sediment transport rate per unit width (i.e., the Einstein number), and τ^* is dimensionless shear stress (i.e., the Shields number). They are defined as,

$$q_s^*=\frac{q_{se}}{\sqrt{RgDD}} \tag{19}$$

$$\tau^*=\frac{\tau_b}{\rho RgD} \tag{20}$$

$$\tau_b=\rho C_f u^2 \tag{21}$$

where D is the characteristic grain size of the bed sediment (here approximated as uniform); τ_b is bed shear stress; and R is submerged specific gravity of sediment, defined as (ρ_s - ρ) / ρ, in which ρ_s is density of sediment, and ρ is density of water. The sediment submerged specific gravity R is specified as 1.65 in this paper, which is an appropriate estimate for natural rivers, and corresponds to quartz.

In the relation of Ma et al. (2017), the dimensionless coefficient α_s = 0.9 and the dimensionless exponent n_s = 1.68. These values are quite different from the original relation of Engelund and Hansen (1967), in which α_s = 0.05 and n_s = 2.5. Ma et al. (2017) demonstrated that such differences imply that the riverbed of the LYR is dominated by low-amplitude bedform features (dunes) approaching upper-regime plane bed. According to this finding, form drag is then neglected in our modeling, and all of the bed shear stress is used for sediment transport.

2.4.2 Sediment mixtures

We implement the relation of Naito et al. (accepted subject to revision) to calculate the equilibrium sediment transport rate of size mixtures. Using field data from the LYR, Naito et al. (accepted subject to revision) extended the Engelund and Hansen (1967) relation to a surface-based grain-size specific form, in which the suspended load transport rate of the *i*-th size range is tied to the availability of this size range on the bed surface:

$$q_{sei} = \frac{N_i^* F_i u_*^3}{RgC_f} \tag{22}$$

where N_i^* is the dimensionless sediment transport rate in the *i*-th size range, and u_* is shear velocity calculated from the bed shear stress τ_b:

$$u_* = \sqrt{\frac{\tau_b}{\rho}} \tag{23}$$

The transport relation itself takes the form,

$$N_i^* = A_i \left(\tau_g^* \frac{D_{sg}}{D_i} \right)^{B_i} \tag{24}$$

in which D_i is the characteristic grain size for sediment in the *i*-th size range, D_{sg} is the geometric mean grain size in the active layer, and τ_g^* is the dimensionless bed shear stress associated with D_{sg}. The parameters τ_g^*, coefficient A_i, and exponent B_i are calculated as,

$$\tau_g^* = \frac{\tau_b}{\rho RgD_{sg}} \tag{25}$$

$$A_i = 0.46 \left(\frac{D_i}{D_{sg}} \right)^{-0.84} \tag{26}$$

$$B_i = 0.35\left(\frac{D_i}{D_{sg}}\right)^{-1.16} \quad (27)$$

If A_i and B_i are specified as constant values in Eq (24), then the sediment transport rate for each size range ~~only~~ depends only on the flow shear stress and the characteristic grain size of this size range, without being affected by other size ranges. But according to Eqs.~~s~~ (26) and (27), the coarser the sediment the smaller the values of A_i and B_i will be, thus leading to ~~a~~ reduced~~smaller~~ mobility for coarse sediment (and increased~~a larger~~ mobility for fine sediment) due to the presence of grains of other sizes. Thus the relations (26) and (27) serve as hiding function that allow for grain sorting. ~~The forms of Eqs. (26) and (27) thus represent~~indicate ~~that the hiding effects between coarse and fine sediment play a role in this sediment transport relation~~.

We note that a form of the Engelund-Hansen equation for mixtures was introduced by Van der Scheer et al. (2002), and implemented by Blom et al. (2016, 2017). This form, however, has no hiding formulation built into it, and is thus not suitable for the LYR.

3. Numerical modeling of the LYR using the two forms of Exner equation

In this section, we conduct numerical simulations using both the flux form and the entrainment form of the Exner equation, with the aim to study under what circumstances the two forms give different predictions. Numerical simulations are conducted in the setting of the LYR. We specify a 200 km long channel reach for our simulations, along with a constant channel width of 300 m and an initial longitudinal slope of 0.0001. Bed porosity λ_p is specified as 0.4. Based on field measurements of the LYR available to us, we implemented a dimensionless Chezy resistance coefficient C_z of 30, which corresponds to a dimensionless bed resistance coefficient C_f of 0.0011. For the entrainment form of Exner equation, we specify the ratio of near bed sediment concentration to flux-averaged sediment concentration r_0 (r_{0i}) = 1. Such a value of r_0 (r_{0i}) corresponds to a vertically uniform profile of sediment concentration, and will thus give a maximum difference between the prediction of entrainment form and the prediction of the flux form. More discussion about the effects of r_0 is~~will be~~ presented in Section 4.3.

A constant flow discharge of 2000 m^3/s (corresponding to a flow discharge per unit width q_w of 6.67 m^2/s) is introduced at the inlet of the channel with the flood intermittency factor I_f estimated as 0.14 (Naito et al., accepted subject to revision). The downstream end is specified far from the river mouth to neglect the effects of backwater. Therefore, the bed elevation is held constant and the water depth is specified as the normal flow depth at the downstream end of the calculational domain. The above flow discharge per unit width q_w combined with the bed slope S as well as the bed resistance coefficient C_f leads to a normal flow depth of 3.69 m. In our simulation, we use the height of bedforms in the LYR to determine the thickness of the active layer (Blom ~~et al.~~, ~~2003~~2008). According to the field survey of Ma et al. (2017), the characteristic height of bedforms in the LYR is about 20% of the normal flow depth, which can fall in the range suggested by the data analysis of

Bradley and Venditti (2017). This eventually leads to an estimate of active layer thickness of L_a = 0.738 m. The sublayer in the substrate to store the vertical stratigraphy is specified with a thickness of 0.5 m.

Two cases are considered here. In the first case, the sediment grain size distribution of LYR is simplified to a uniform grain size of 65 μm. This is based on the measured grain size distribution of bed material at the Lijin gauging station, which has a median grain size of D_{50} = 66.6 μm, ~~and~~ a geometric mean grain size of D_g = 65.5 μm, and a geometric standard deviation σ_g = 2.0, as shown in Fig. 1(c). In the second case, we consider the effects of sediment mixtures. The grain size distribution of the initial bed is based on the bed material at the Lijin gauging station, as shown in Fig. 1(c), but we renormalize the measured grain size distribution with a cutoff for washload at 15 μm as suggested by Ma et al. (2017). The renormalized grain size distribution for the initial bed as implemented in the case of sediment mixtures is shown in Fig. 2, with a total number of grain size fractions of 5~~.~~. The sediment porosity λ_p is taken as 0.4 in this paper. In both the two cases, simulations start with an equilibrium state where sediment supply rate, ~~=~~ sediment transport rate, and ~~=~~ equilibrium sediment transport rate being the same, so that the initial state of the channel is in equilibrium. Then we cut the sediment supply rate (of each size range) to only 10% of the equilibrium sediment transport rate and keep this sediment supply rate. This is to mimic the reduction of sediment load in the LYR in recent years, as shown in Fig. 1(b). The grain size distribution of sediment supply in the case of sediment mixtures is shown in Fig. 2.

The 200 km channel reach is discretized into 401 cells, with cell size Δx of 500 m. In the case of uniform sediment, we specify a time step for morphologic calculation $\Delta t_m = 10^{-4}$ year and a time step for hydraulic calculation $\Delta t_h = 10^{-6}$ year. In the case of sediment mixtures, we specify a time step for morphologic calculation $\Delta t_m = 10^{-5}$ year, and a time step for hydraulic calculation $\Delta t_h = 10^{-6}$ year. Computational conditions are briefly summarized in Table 1. The computational conditions we implement are much simpler than the rather complicated conditions of the actual LYR. But it should be noted that the aim of this paper is not to reproduce specific aspects of the morphodynamic processes of LYR, but to compare the flux form and entrainment form of Exner equation in the context of conditions typical of LYR.

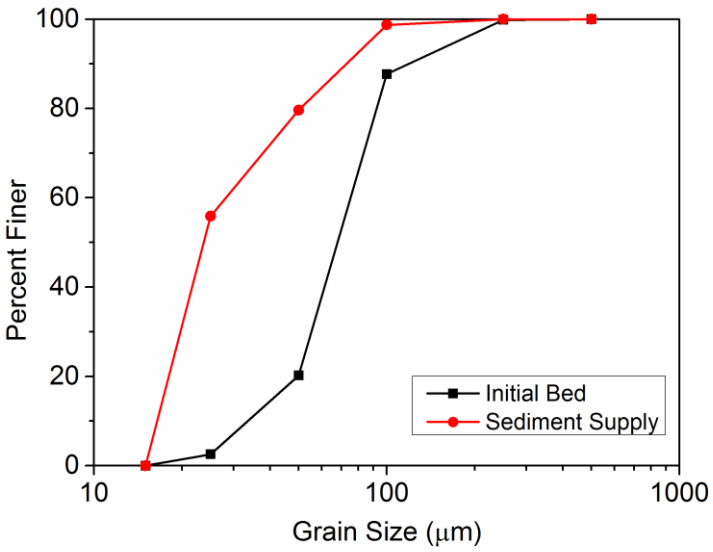

Figure 2. Grain size distributions of both the initial bed and the sediment supply in the case of sediment mixtures. For the initial bed, the surface and substrate grain size distributions are the same. The grain size distribution of the initial bed is renormalized based on the field data at the Lijin gauging station. The grain size distribution of the sediment supply equals to the grain size distribution of bed material load at equilibrium. Grain sizes in the range of washload ~~Washload sizes~~ have been removed from both distributions.

Table 1. Summary of computational conditions for numerical modeling of the LYR.

Parameter	Value
Channel length L	200 km
Channel width B	300 m
Initial slope S_I	0.0001
Dimensionless Chezy resistance coefficient C_z	30
Flow discharge per unit width q_w	6.67 m^2/s
Flood intermittency factor I_f	0.14
ratio of near bed concentration to average concentration r_0 (r_{0i})	1
Characteristic grain size in the case of uniform sediment	65 μm
Submerged specific gravity of sediment R	1.65
Porosity of bed deposits λ_p	0.4
cell size Δx	500 m
time step for morphologic calculation Δt_m	10^{-4} year (uniform sediment) 10^{-5} year (sediment mixtures)
time step for hydraulic calculation Δt_h	10^{-6} year

3.1 Case of uniform sediment

In this case, we implement a uniform grain size of 65 μm for both the bed material and sediment supply. Such a grain size is nearly equal to the observed median grain size (or geometric mean grain size) of bed material at Lijin gauging station. The relation of Ma et al. (2017) is implemented to calculate the transport rate of bed material suspended load. This relation provides an equilibrium sediment transport rate per unit width q_{se} of 0.0136 m^2/s under the given flow discharge, bed slope and sediment grain size. With a flood intermittency factor I_f of 0.14, this further gives a mean annual bed material load of 47.8 Mt/a. Adding in washload according to the estimate of Naito et al. (accepted subject to revision), total mean annual load is 86.9 Mt/a, a value that is of the same order of magnitude as averages over the period 2000-2016 (89-126 Mt/a depending on site), i.e. since the operation of Xiaolangdi Dam in 1999 (Fig. 1(b)). The sediment supply rate q_{sf} we specify at the upstream end of the channel is only 10% of the equilibrium sediment transport rate (i.e. sediment supply rate is cut by 90% from the equilibrium state), such that q_{sf} = 0.00136 m^2/s.

Figure 3 shows the modeling results using the flux form of the Exner equation. As we can see in the figure, the bed degrades and the sediment load decreases in response to the cutoff of sediment supply. Such adjustments start from the upstream end of the channel and gradually migrate downstream. Figure 4 shows the modeling results using the entrainment form of Exner equation. A comparison between Fig. 4 and Fig. 3 shows that the entrainment form and the flux form give very similar predictions in this case. The entrainment form provides a somewhat slower degradation (at the upstream end the flux form predicts a 3-m degradation whereas the entrainment form predicts a 2.3-m degradation) and a more diffusive sediment load reduction. Such more diffusive predictions of sediment load variation can be ascribed to the condition~~cept~~ of nonequilibrium transport that is embedded in the entrainment form. This issue will be studied analytically in Section 4. Here we present the results for~~of~~ only 0.2 year after the cutoff of sediment supply, since the differences between the predictions of the two forms tend to be the most evident shortly after the disruption but gradually diminish as the river approaches the new equilibrium (El kadi Abderrezzak and Paquier, 2009). Modeling results over a longer time scale will be discussed in Section 4.3.

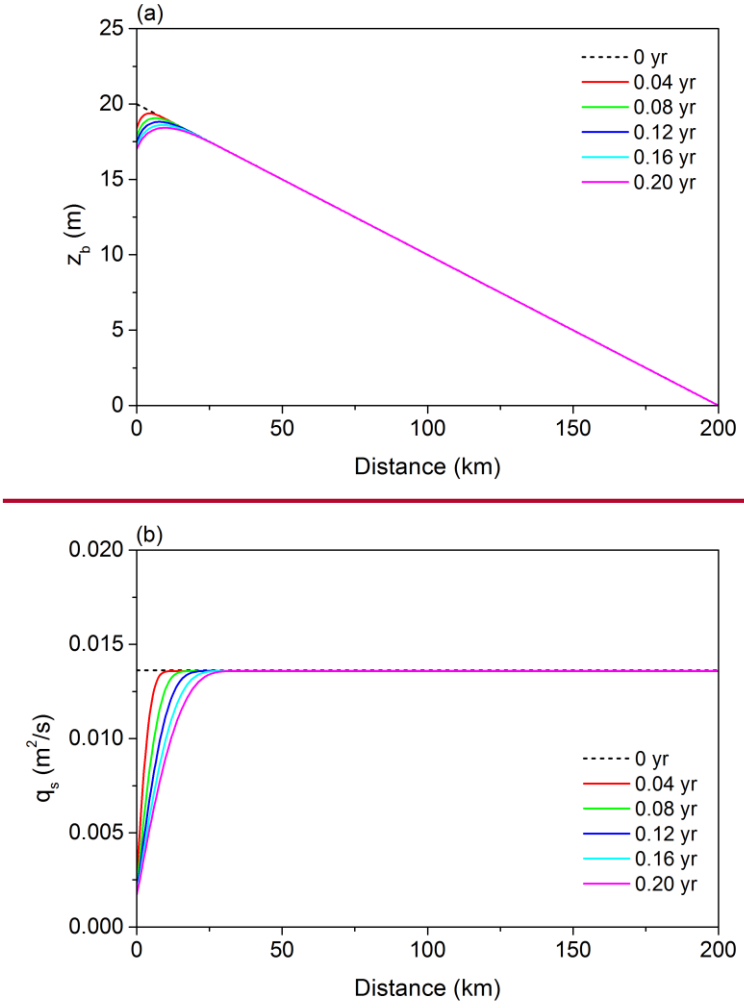
(a)
25
20
15
10
5
0
z_b (m)
0
50
100
150
200
Distance (km)
0 yr
0.04 yr
0.08 yr
0.12 yr
0.16 yr
0.20 yr
(b)
0.020
0.015
0.010
0.005
0.000
q_s (m^2/s)
0
50
100
150
200
Distance (km)
0 yr
0.04 yr
0.08 yr
0.12 yr
0.16 yr
0.20 yr

349

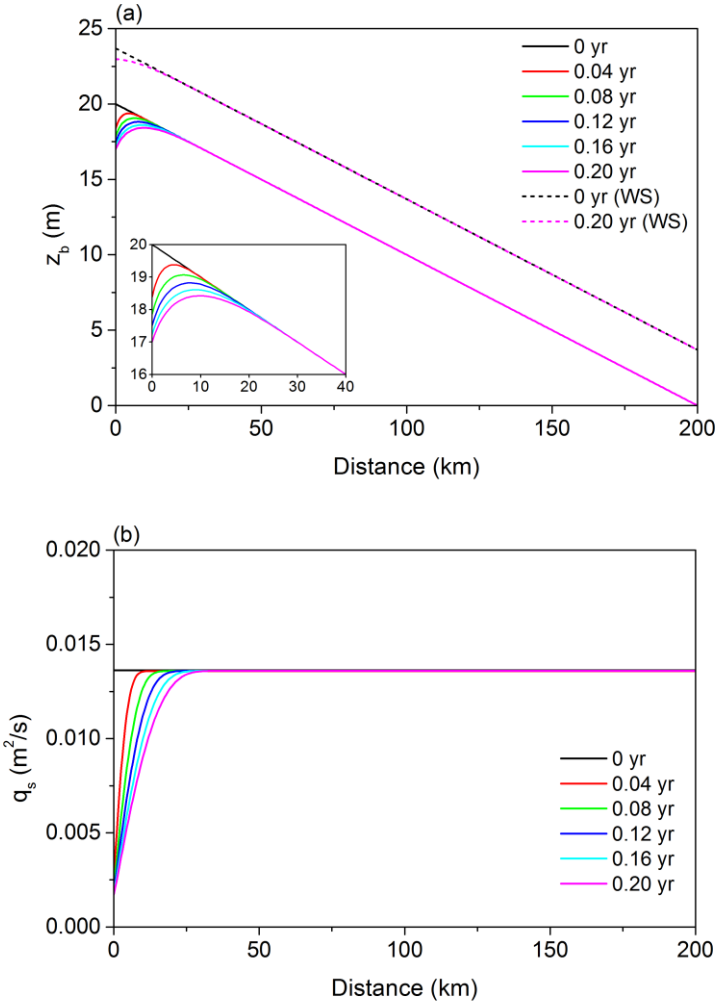

Figure 3. 0.2 year results for the case of uniform sediment using the flux form of Exner equation: time variation of (a) bed elevation z_b and water surface (WS), (b) sediment load per unit width q_s of the LYR in response to the cutoff of sediment supply. The inset shows detailed results near the upstream end.

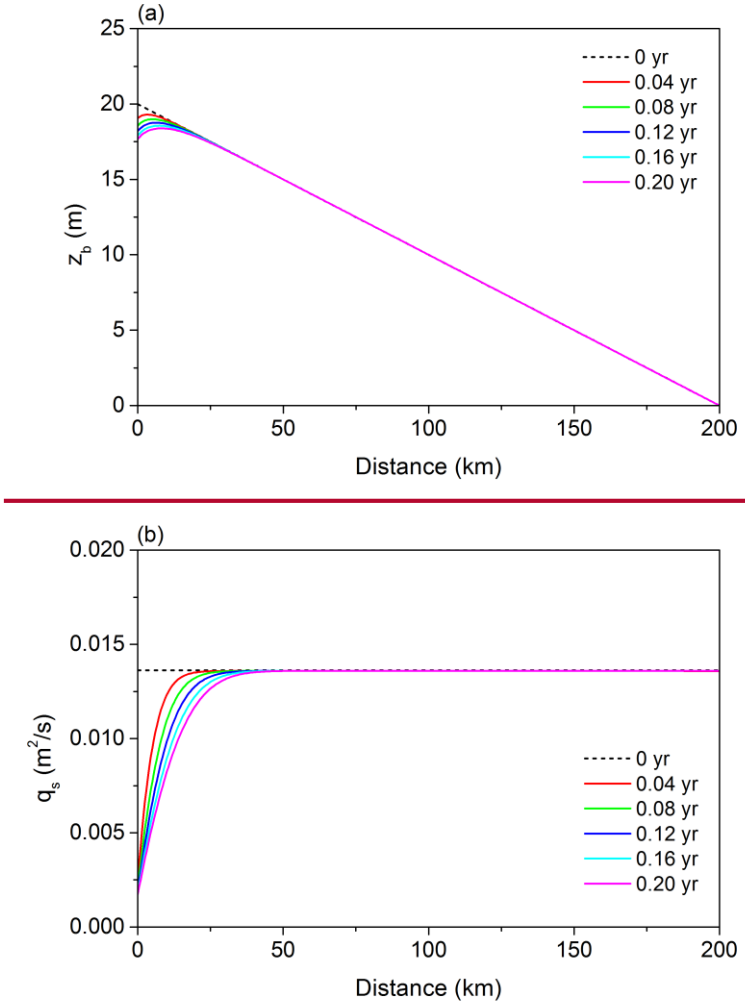
(a)
25
20
15
10
5
0
z_b (m)
0
50
100
150
200
Distance (km)
0 yr
0.04 yr
0.08 yr
0.12 yr
0.16 yr
0.20 yr
(b)
0.020
0.015
0.010
0.005
0.000
q_s (m^2/s)
0
50
100
150
200
Distance (km)
0 yr
0.04 yr
0.08 yr
0.12 yr
0.16 yr
0.20 yr

354

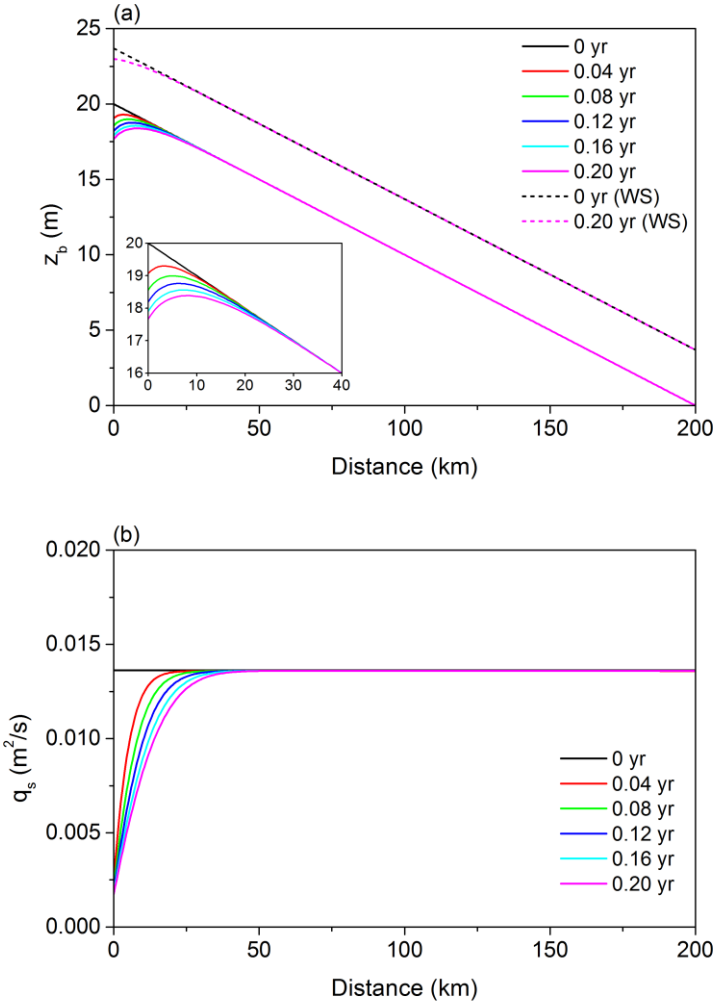

Figure 4. 0.2 year results for the case of uniform sediment using the entrainment form of Exner equation: time variation of (a) bed elevation z_b and water surface (WS), (b) sediment load per unit width q_s of the LYR in response to the cutoff of sediment supply. The inset shows detailed results near the upstream end.

To further quantify the differences between the predictions of the two forms, we propose the following normalized parameter,

$$\delta(y) = \left| \frac{y_E - y_F}{y_F} \right| \times 100\% \tag{28}$$

where y denotes an arbitrary variable calculated by the morphodynamic model, and subscripts F and E denote results using the flux form and the entrainment form respectively. Therefore, $\delta(y)$ denotes the difference between the prediction the two forms y_F and y_E normalized by the prediction of the flux form y_F.

Table 2 gives a summary of the maximum values of δ along the channel at different times in the case of uniform sediment. The values of δ for both z_b and q_s are presented. As we can see from the table, the maximum value of $\delta(z_b)$ along the calculational domain stayskeeps within 4% in the first 0.2 year after the cutoff of sediment supply. This indicates that the flux form and the entrainment form can indeed give almost the same prediction in terms of bed elevation in this case. But in the case of the sediment load per unit width q_s, the maximum value of $\delta(q_s)$ can be as high as 20%, indicating that even though the two forms give qualitatively similar patterns of evolution in terms of sediment load as shown in Figs. 3 and 4, athe quantitative difference iscan be clearly evident due to the more diffusive nature of the predictions of the entrainment form. The value of $\delta(q_s)$ is largest at the beginning of the simulation, and then gradually reduces with time.

Table 2. Quantification of the difference between predictions of the flux form and the entrainment form in the case of uniform sediment. The maximum values of $\delta(z_b)$ and $\delta(q_s)$ in the calculational domain are presented every 0.04 year.

		0.04 yr	0.08 yr	0.12 yr	0.16 yr	0.20 yr
original v_s	$\delta(z_b)$	3.66 7 %	3.91 %	3.93 %	3.88 9 %	3.81 %
	$\delta(q_s)$	20.48 5 %	15.11 %	12.31 %	10.48 5 %	9.17 2 %
v_s multiplied by 0.05	$\delta(z_b)$	8.23 %	10.94 %	12.66 7 %	13.92 %	14.91 %
	$\delta(q_s)$	74.83 %	68.14 %	63.04 %	58.89 9 %	55.41 %

The above results show that the flux form and the entrainment form can provide similar predictions of LYR when the bed sediment grain size distribution is simplified to a uniform value of 65 μm. To understand under what conditions the two forms will lead to more different results, we conduct an idealized run using the entrainment form in which the sediment fall velocity v_s is arbitrarily multiplied by a factor of 0.05. That is to say, we keep the sediment grain size at 65 μm in the computation of the Shields number, but let the sediment fall velocity in Eqs. (8) and (10) equal only 1/20 of the value calculated by the relation of Dietrich (1982) from this grain size. With a much smaller, and indeed intentionally unrealistic sediment fall velocity, the entrainment form predicts very different results as shown in Fig. 5. The adjustments of the sediment load become even more diffusive in space: it almost takes almost the entire 200 km reach for the sediment load to adjust from the upstream disruption to the equilibrium transport rate. Meanwhile, there is barely any bed degradation at the upstream end after 0.2 year, in correspondence with the fact that the spatial gradient of q_s becomes quite small. In Table 2 we also exhibit the δ values for this idealized run. It is no surprise that both $\delta(z_b)$ and $\delta(q_s)$ are high, as the entrainment form and flux form predict very different patterns with such an arbitrarily reduced sediment fall velocity.

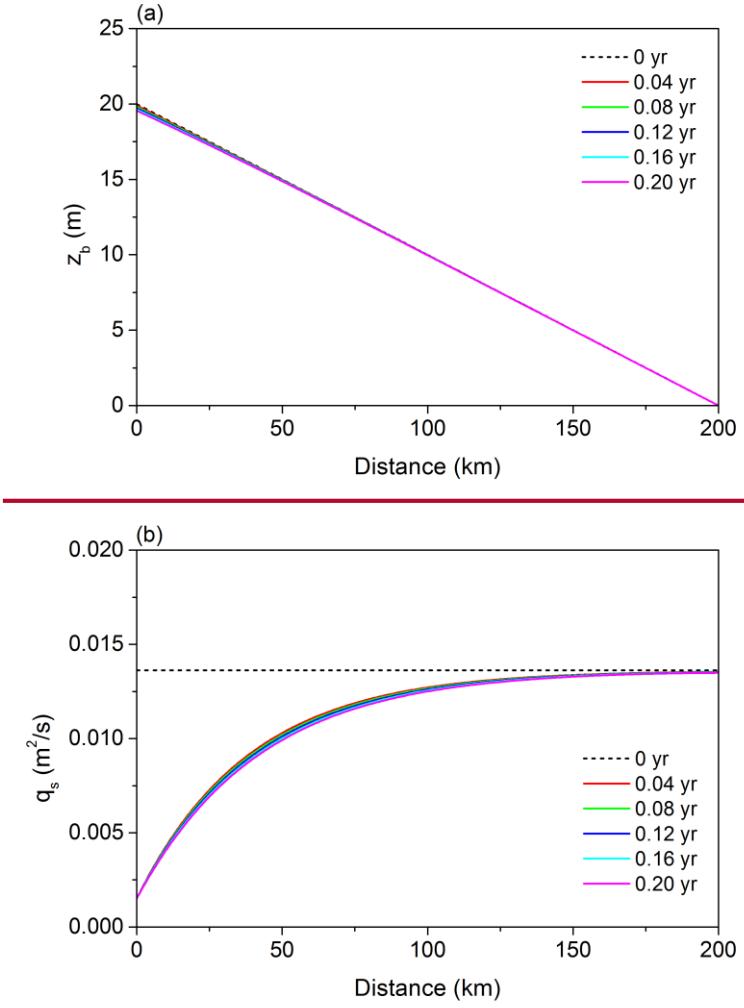
(a)
25
20
15
10
5
0
z_b (m)
0
50
100
150
200
Distance (km)
0 yr
0.04 yr
0.08 yr
0.12 yr
0.16 yr
0.20 yr
(b)
0.020
0.015
0.010
0.005
0.000
q_s (m^2/s)
0
50
100
150
200
Distance (km)
0 yr
0.04 yr
0.08 yr
0.12 yr
0.16 yr
0.20 yr

388

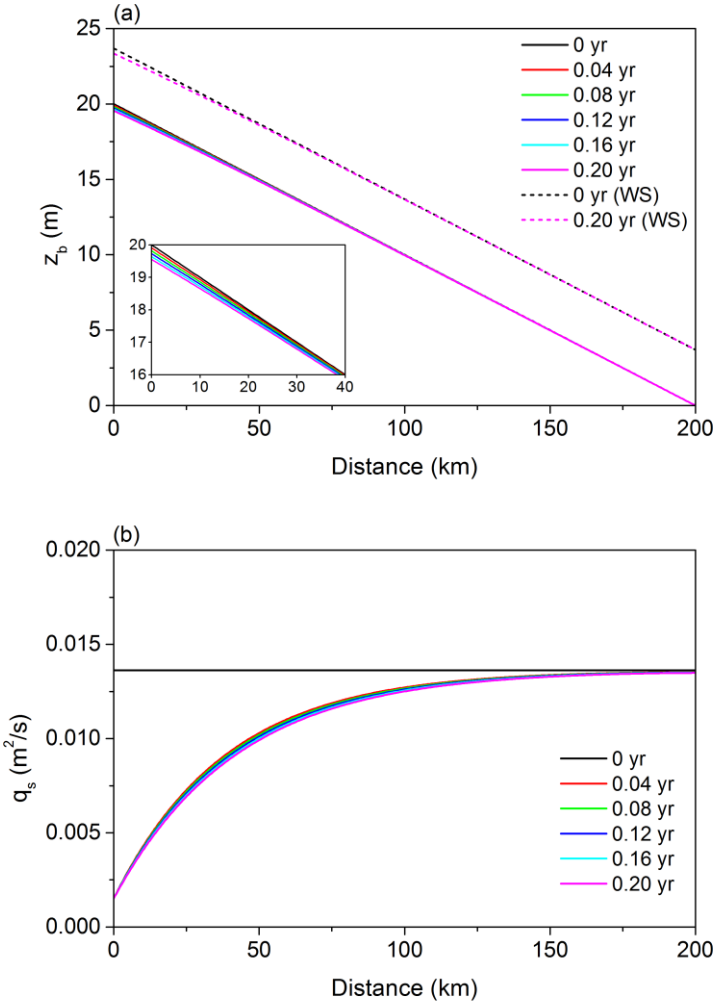

Figure 5. 0.2 year results for the case of uniform sediment using the entrainment form of Exner equation: time variation of (a) bed elevation z_b and water surface (WS), (b) sediment load per unit width q_s of the LYR in response to the cutoff of sediment supply. Sediment fall velocity v_s is arbitrarily multiplied by a factor of 0.05 while holding bed grain size constant in this run. The inset shows detailed results near the upstream end.

In Section 3.1 of the main text, we compare the flux-based morphodynamics and entrainment-based morphodynamics of uniform sediment, under constant water discharge and sediment supply. The aim is to focus on the comparison of the two formulations without being distracted by the complexity of boundary conditions. In Section S2 of the Supplement ~~Information~~, we also conduct numerical simulations with ~~under~~ hydrographs. Results indicate that our conclusions based on constant flow discharge also hold when hydrographs are considered: the flux-form and the entrainment form (with the sediment fall velocity not adjusted) of the Exner equation give very similar prediction using ~~with~~ a characteristic grain size of 65 μm.

3.2 Case of sediment mixtures

In this section we consider the morphodynamics of sediment mixtures rather than the case of a uniform bed grain size implemented in section 3.1. The grain size distribution of the initial bed is based on field data at the Lijin gauging station, and is shown in Fig. 2. Using the sediment transport relation of Naito et al. (accepted subject to revision) for mixtures, such a grain size distribution combined with the given bed slope and flow discharge leads to a total equilibrium sediment transport rate per unit width q_{seT} of 0.0272 m^2/s. With a flood intermittency factor I_f of 0.14, this further gives a mean annual bed material load of 95.5 Mt/a. Adding in washload according to the estimate of Naito et al. (accepted subject to revision), total mean annual load 173.7 Mt/a, a value that is of the same order of magnitude as averages over the period 2000-2016 (89-126 Mt/a depending on site), i.e. since the operation of Xiaolangdi Dam in 1999 (Fig. 1(b)). The sediment supply rate of each grain size range is set at 10% of its equilibrium sediment transport rate. This results in a total sediment supply rate of q_{sf} = 0.00272 m^2/s, and a grain size distribution of the sediment supply (shown in Fig. 2) that is identical to the grain size distribution of the equilibrium sediment load before the cutoff. That is, the grain size distribution of sediment supply does not change, only the total sediment supply is reduced by 90%. Again we exhibit simulation results for only 0.2 year here, a value that is enough to show the differences between the two forms, flux and entrainment, as applied to mixtures. Modeling results over a longer time scale are presented in Section 4.3.

Figure 6 shows the simulation results using the flux form of the Exner equation. As a result of the reduced sediment supply at the inlet, bed degradation occurs first at the upstream end and then gradually migrates downstream. The total sediment transport rate per unit width q_{sT} also reduces as a response to the cutoff of sediment supply. More specifically, the evolution of q_{sT} shows marked evidence of advection, with at least two kinematic waves being observed within 0.2 year. Actually as illustrated by Stecca et al. (2014, 2016), each grain size fraction shwould induce athe migratingon of a wave. As shown in Fig. 6(b), the fastest kinematic wave migrates beyond the 200 km reach within 0.06 year, and the second fastest kinematic wave migrates for a distance of about 60 km in 0.2 year. Figures 6(c) and 6(d) show the results for the surface geometric mean grain size D_{sg} and geometric mean grain size of suspended load D_{lg} respectively. As can be seen therein, both the bed surface and the suspended load coarsen as a result of the cutoff of sediment supply This represents armoring, mediated by the hiding functions of Eqs. (26) and (27). Such coarsening is not evident near the upstream end, possibly due to the inverse slope visible in Fig. 6(a). Similarly to the variation of q_{sT}, the patterns of time variation of both D_{sg} and D_{lg} also exhibit very clear kinematic waves, with migration rates about the same as those of $q_{sT.}$

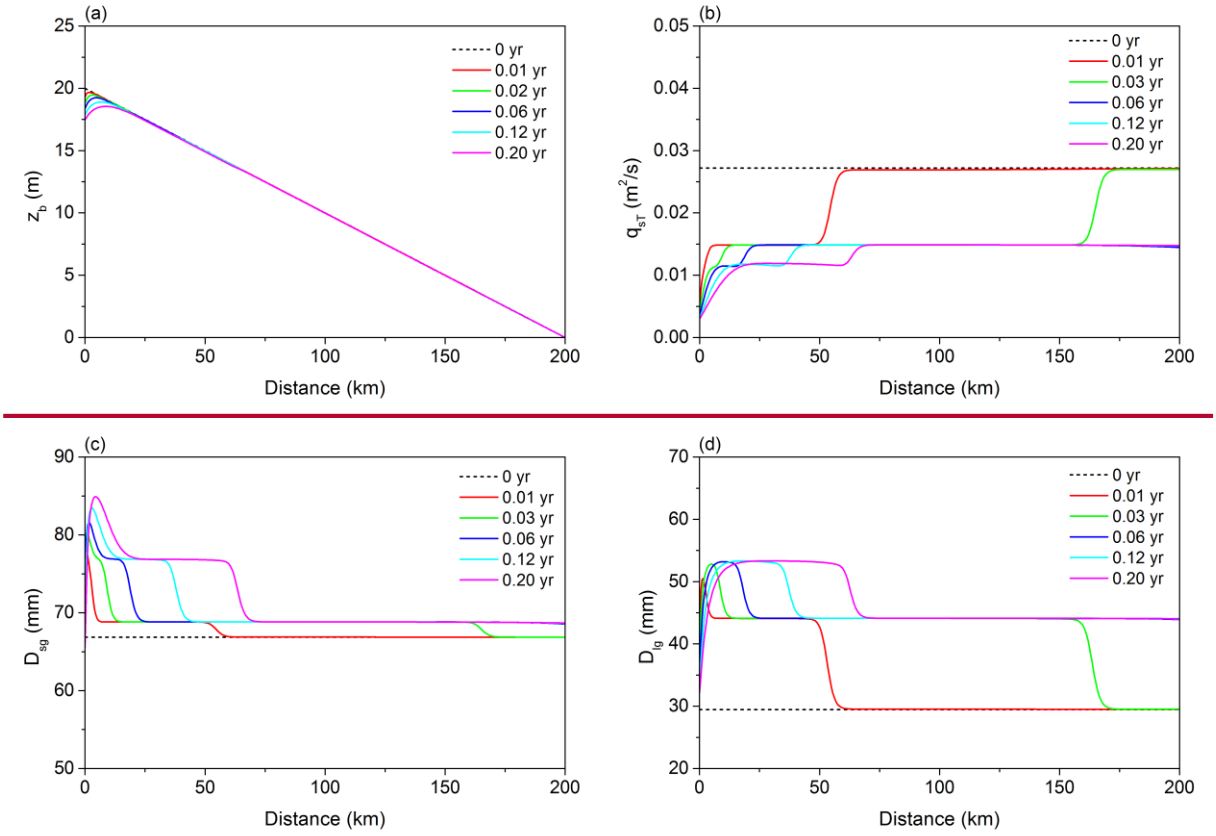
(a)
z_b (m)
Distance (km)
0 yr
0.01 yr
0.02 yr
0.06 yr
0.12 yr
0.20 yr
(b)
q_{sT} (m^2/s)
Distance (km)
0 yr
0.01 yr
0.03 yr
0.06 yr
0.12 yr
0.20 yr
(c)
D_{sg} (mm)
Distance (km)
0 yr
0.01 yr
0.03 yr
0.06 yr
0.12 yr
0.20 yr
(d)
D_{lg} (mm)
Distance (km)
0 yr
0.01 yr
0.03 yr
0.06 yr
0.12 yr
0.20 yr

428

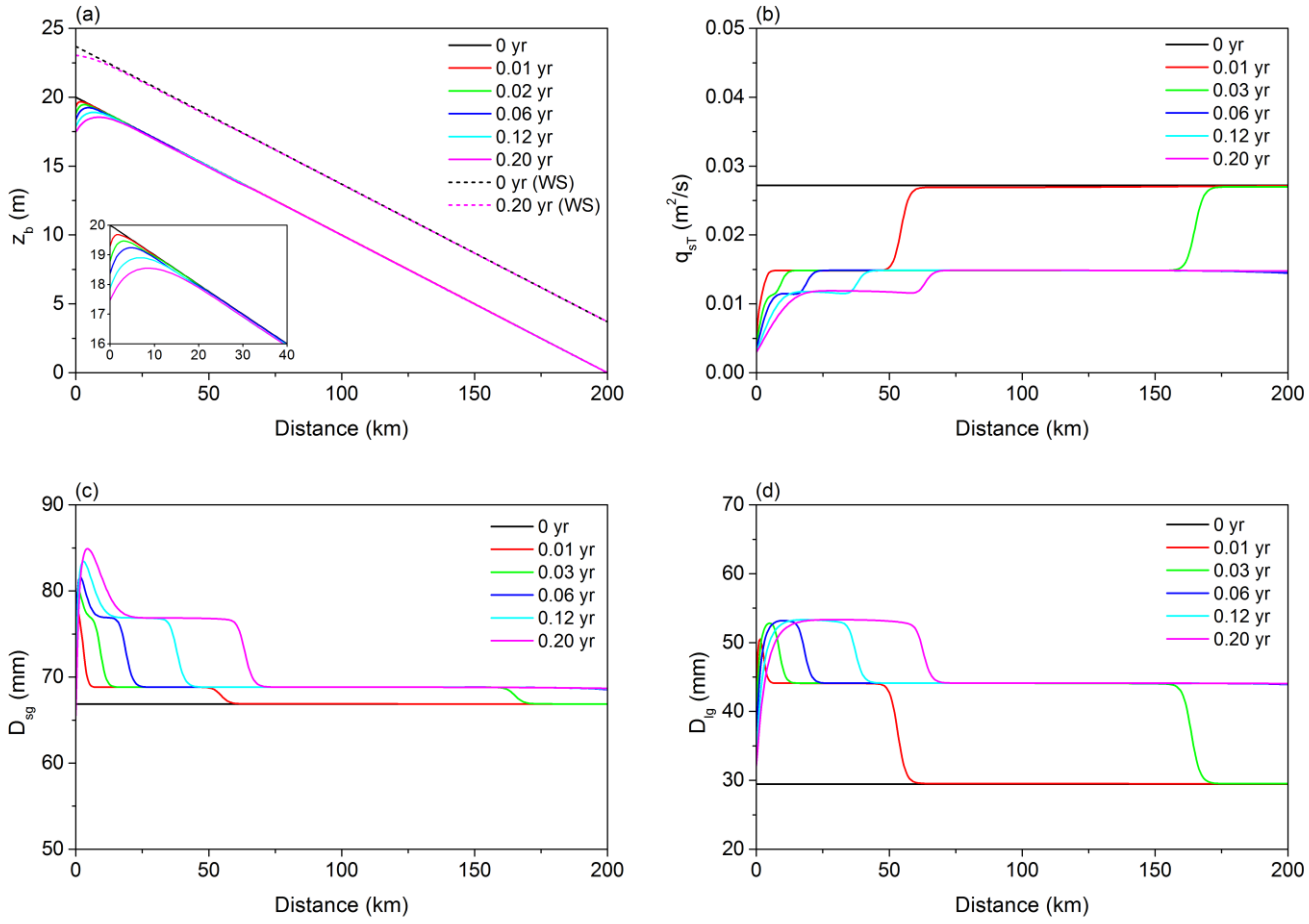

Figure 6. 0.2 year results for the case of sediment mixtures using the flux form of Exner equation: time variation of (a) bed elevation z_b, and water surface (WS), (b) total sediment load q_{sT}, (c) surface geometric mean grain size D_{sg} and (d) geometric mean grain size of sediment load of the LYR in response to the cutoff of sediment supply. The inset shows detailed results near the upstream end.

Figure 7 shows the simulation results obtained using the entrainment form of the Exner equation. In general, the patterns of variation predicted by the entrainment form have similar trends and magnitudes to those predicted by the flux form: the bed degrades near the upstream end, the suspended load transport rate reduces in time, and both the bed surface and the suspended load coarsen as a result of the cutoff of sediment supply. But the results based on the two forms exhibit very evident differences when multiple grain sizes are included. That is, the results predicted by the entrainment form are sufficiently diffusive so that the variations of q_{sT}, D_{sg}, and D_{lg} (Figs. 7(b), 7(c) and 7(d)) do not show the advective character seen in Fig. 6. Figure 7c, however, shows the same armoring as in the case of calculations with the flux form. No clear kinematic waves can be observed in Fig. 7. Table 3 gives a summary of the values of δ in the case of sediment mixtures. The prediction of bed

elevation is not affected much when multiple grain sizes are considered, with $\delta(\underline{z_b})$ being no more than 3.5% within 0.2 year. The δ values of q_{sT}, D_{sg}, and D_{lg} are, however, relatively large since the two forms predict quite different patterns of variations, as shown in Fig. 6 and Fig. 7.

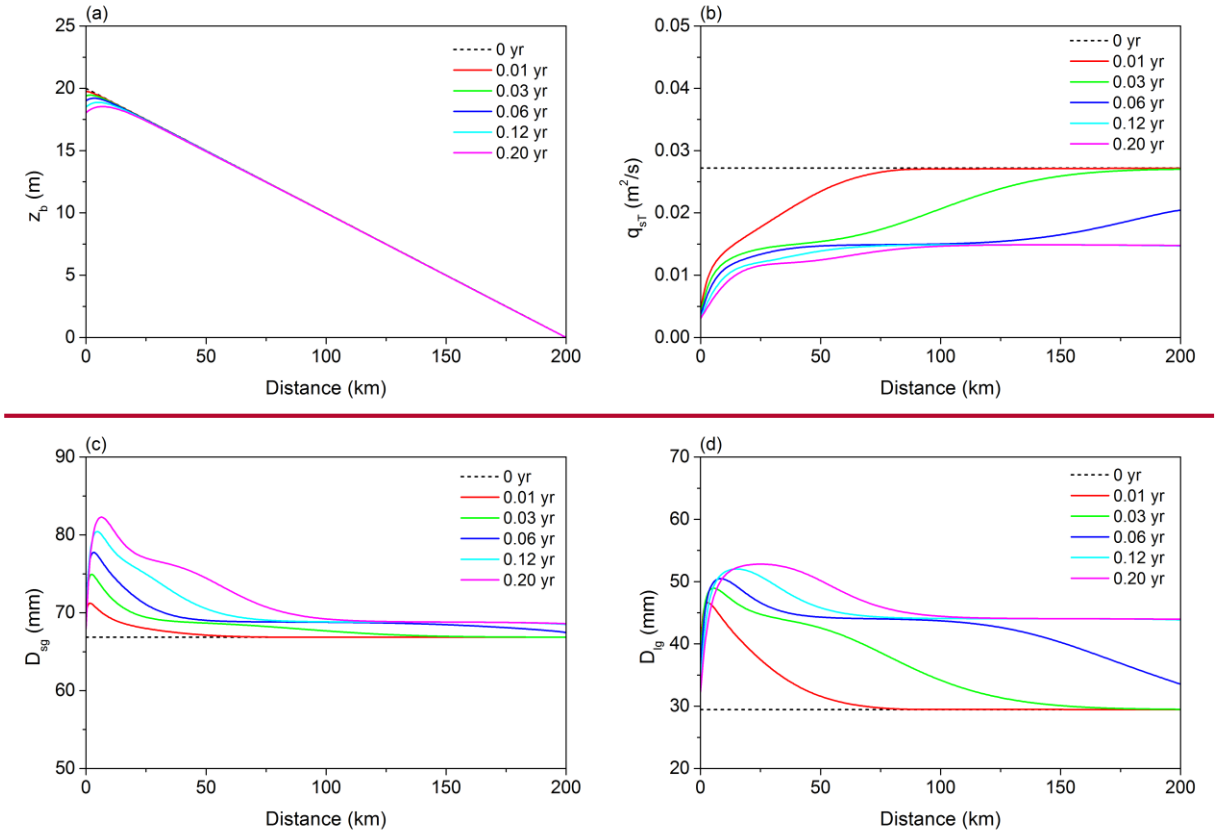

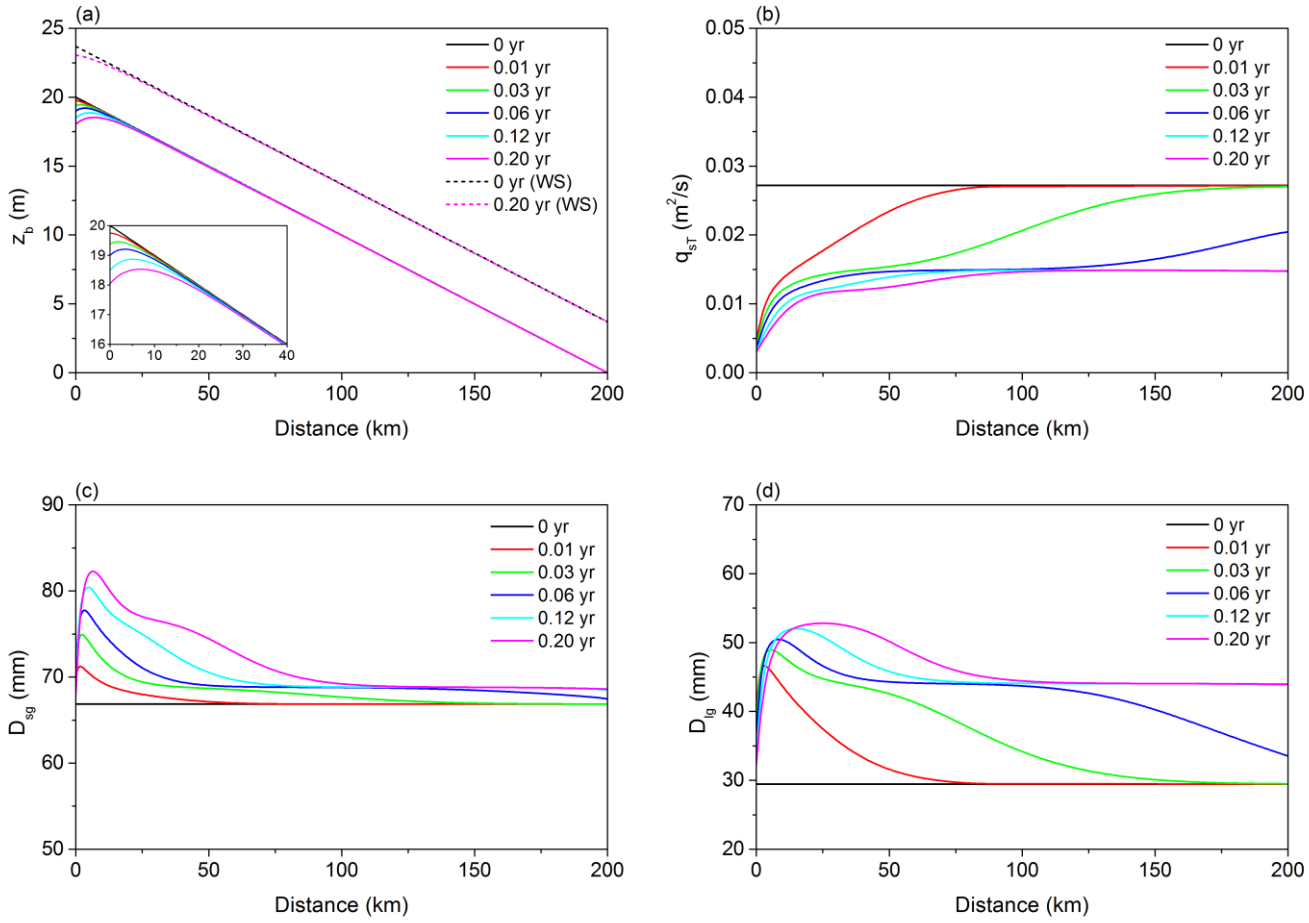

Figure 7. 0.2 year results for the case of sediment mixtures using the entrainment form of Exner equation: time variation of (a) bed elevation z_b~~,~~ and water surface (WS), (b) total sediment load q_{sT}, (c) surface geometric mean grain size D_{sg} and (d) geometric mean grain size of sediment load of the LYR in response to the cutoff of sediment supply. The i~~I~~nset shows ~~the~~ detailed results near the upstream end.

Table 3. Quantification of the difference between predictions of the flux form and the entrainment form in the case of sediment mixtures. The maximum values of δ in the calculational domain are presented at different times.

		0.01 yr	0.03 yr	0.06 yr	0.12 yr	0.20 yr
original v_s	$\delta(z_b)$	2.3~~1~~ %	3.2~~15~~ %	3.4~~4~~ %	3.4~~4~~ %	3.2~~4~~ %
	$\delta(q_{sT})$	54.~~66~~ 7 %	76.1~~1~~ %	41.1~~3~~ %	10.~~45~~ 5 %	11.~~77~~ 8 %
	$\delta(D_{sg})$	10.~~07~~ 1 %	8.6~~0~~ %	7.~~18~~ 2 %	6.0~~2~~ %	5.4~~0~~ %
	$\delta(D_{lg})$	27.1~~0~~ %	31.~~87~~ 9 %	23.~~67~~ 7 %	7.~~16~~ 2 %	7.~~68~~ 7 %
v_s multiplied by 20	$\delta(z_b)$	0.~~27~~ 3 %	0.4~~0~~ %	3.8~~3~~ %	0.~~26~~ 3 %	0.2~~1~~ %
	$\delta(q_{sT})$	81.1~~2~~ %	82.~~26~~ 3 %	39.~~65~~ 7 %	7.~~15~~ 2 %	9.~~28~~ 3 %
	$\delta(D_{sg})$	2.8~~1~~ %	2.8~~4~~ %	~~1.96~~2.0 %	2.~~65~~ 7 %	3.4~~1~~ %

$\delta(D_{lg})$	32.~~78~~ 8 %	33.1~~1~~ %	25.1~~3~~ %	4.~~77~~ 8 %	6.0~~2~~ %

The results shown in Fig. 8 have also been calculated using the entrainment form of the Exner equation, but here the sediment fall velocities v_{si} used in Eqs. (14)-(16) are arbitrarily multiplied by a factor of 20. That is, we still apply the grain size distribution in Fig. 2, but the sediment fall velocities implemented in the simulation are 20 times the corresponding fall velocities calculated by the relation of Dietrich (1982). In the case of uniform sediment in Section 3.1, we arbitrarily reduce the sediment fall velocity to force a difference between the predictions from the entrainment form and those from the flux form. Here we arbitrarily increase the sediment fall velocity with the aim of determining under what conditions the sorting patterns predicted by the two forms converge. As we can see in Fig. 8, with such a larger and intentionally unrealistic sediment fall velocity, the general trend of variations predicted by the entrainment form does not change, but the results show a notably less diffusive pattern. The variations of q_{sT}, D_{sg}, and D_{lg} show more advection compared with Fig. 7, and at least two kinematic waves appear within 0.2 year. It should be noted that even though these kinematic waves appear after we arbitrarily increase the sediment fall velocity, they are more diffusive than those obtained from the flux formulation and also migrate with a slower celerity as compared with those predicted by the flux form, especially for the fastest kinematic wave in the modeling results.

Table 3 summarizes the δ values for this run. The values of $\delta(z_b)$ become smaller with arbitrarily increased sediment fall velocities except for t = 0.06 year. A relatively large value of $\delta(z_b)$ at t = 0.06 year occurs near the downstream end of the channel, where the entrainment form predicts some slight degradation. Also, $\delta(q_{sT})$ is quite large at t = 0.01 year and 0.03 year, even though the results for the case of increased fall velocities become qualitatively more similar to the prediction of the flux form. This is because the flux form and the entrainment form with arbitrarily increased sediment fall velocities predict different celerities for the fastest kinematic wave. The error $\delta(q_{sT})$ becomes smaller from t = 0.06 year as the fastest kinematic wave migrates beyond the channel reach. The error $\delta(D_{lg})$ behaves similarly to $\delta(q_{sT})$, with $\delta(D_{lg})$ being quite large at t = 0.01 year and 0.03 year near the fastest kinematic wave, but gradually becoming smaller as time passes. The error $\delta(D_{sg})$ stays low within the whole 0.2–year period, possibly because the fastest kinematic wave of D_{sg} has a small magnitude, as shown in Fig. 8(c).

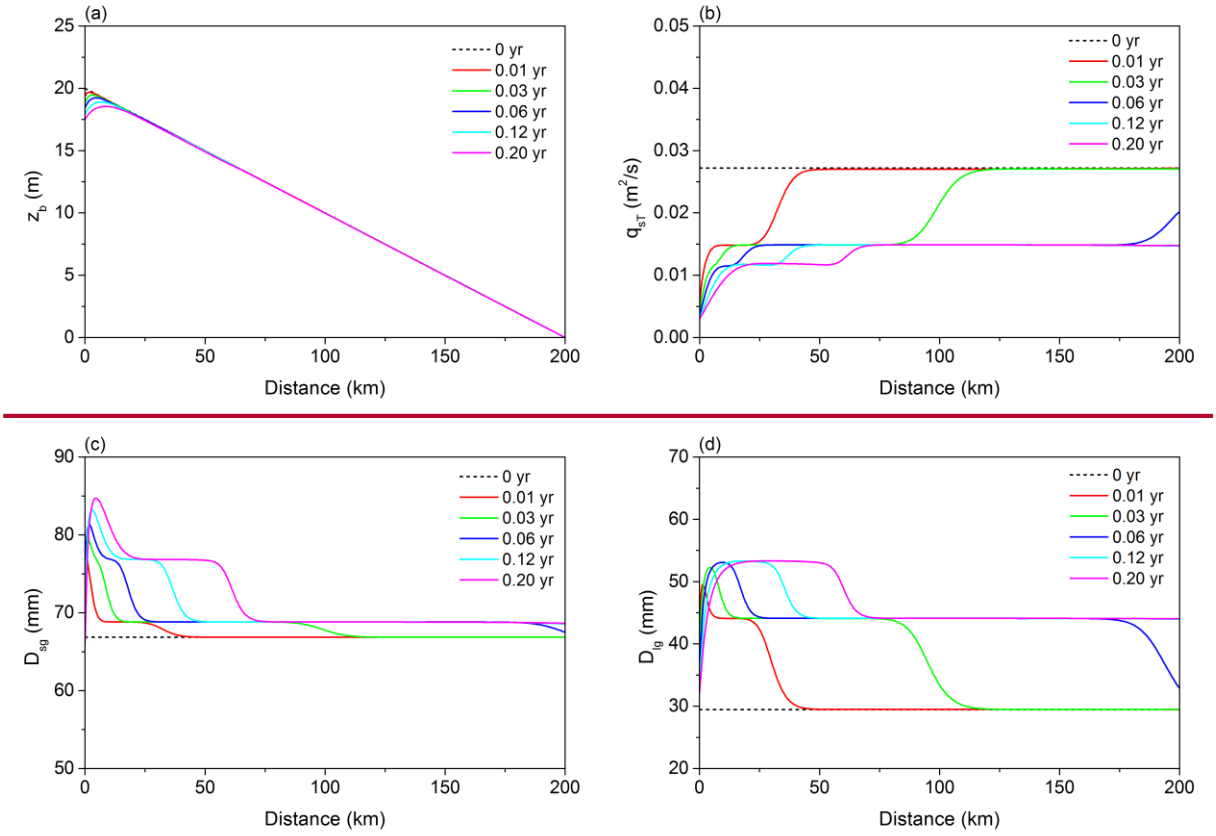
(a)
z_b (m)
Distance (km)
0 yr
0.01 yr
0.03 yr
0.06 yr
0.12 yr
0.20 yr
(b)
q_{sT} (m^2/s)
Distance (km)
(c)
D_{sg} (mm)
Distance (km)
(d)
D_{lg} (mm)
Distance (km)

476

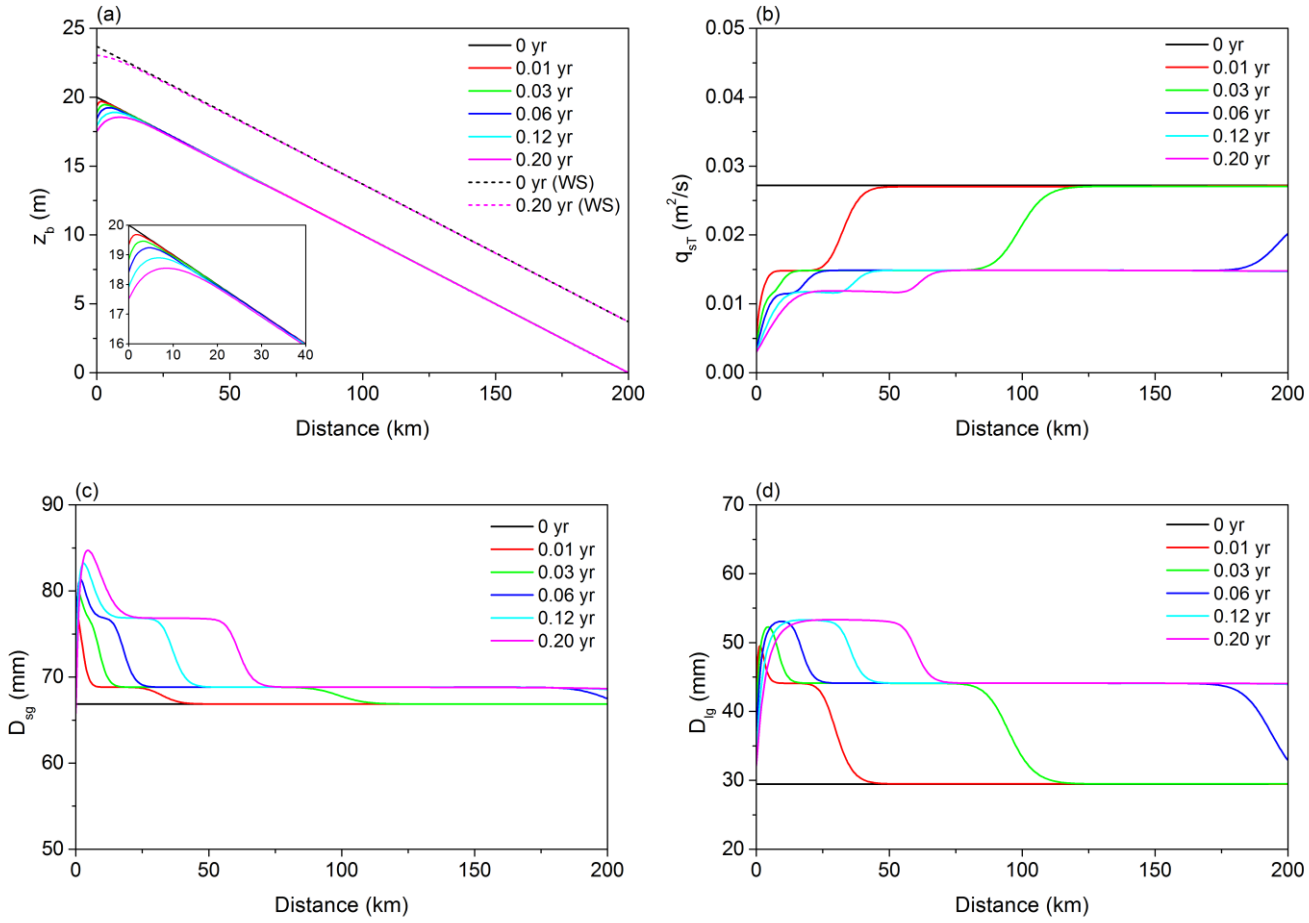

Figure 8. 0.2 year results for the case of sediment mixtures using the entrainment form of Exner equation: time variation of (a) bed elevation z_b~~,~~ and water surface (WS), (b) total sediment load q_{sT}, (c) surface geometric mean grain size D_{sg} and (d) geometric mean grain size of sediment load of the LYR in response to the cutoff of sediment supply. Sediment fall velocities v_{si} are arbitrarily multiplied by a factor of 20 in this run while keeping the grain sizes invariant. The i~~I~~nset shows ~~the~~ detailed results near the upstream end.

In Section S3 of the Supplement ~~Information~~, we conduct additional numerical cases which are similar to the cases in this section, except that hydrographs are implemented instead of constant discharge. Results indicate that our conclusions based on constant flow discharge also hold when hydrographs are considered. The flux ~~-~~form and the entrainment form (with the sediment fall velocity not adjusted) of the Exner equation predict quite different patterns of grain sorting, with the flux form exhibitings~~s~~ more advective character than the entrainment form.

4. Discussion

4.1 Adjustment of sediment load and the adaptation length

In Section 3.1, our simulation shows that in the case of uniform sediment, the flux form and the entrainment form of the Exner equation give very similar predictions for a given sediment size of 65 μm. However, if we arbitrarily reduce the sediment fall velocity by a multiplicative factor of 0.05, the prediction given by the entrainment form will become much more diffusive, in terms of both z_b and q_s. The diffusive nature of the entrainment form as well as the important role played by the sediment fall velocity can be explained in terms of the governing equation.

In the entrainment form, the equation governing suspended sediment concentration is,

$$\frac{1}{I_f}\frac{\partial(hC)}{\partial t}+\frac{\partial(huC)}{\partial x}=v_s\left(E-r_0C\right) \tag{29}$$

i.e. the same as Eq. (10). The sediment transport rate per unit width $q_s = huC = q_wC$, and the dimensionless entrainment rate $E= r_0q_{se}/q_w$. In order to simplify the mathematical analysis, here~~I~~ we consider only the adjustment of sediment concentration in space and neglect the temporal derivative in Eq. (29), so that we get

$$\frac{\partial q_s}{\partial x}=v_s\left(E-r_0C\right)=\frac{1}{L_{ad}}\left(q_{se}-q_s\right) \tag{30}$$

$$L_{ad}=\frac{q_w}{v_s r_0} \tag{31}$$

where L_{ad} can be identified as the adaptation length for suspended sediment to reach equilibrium. This definition of adaptation length is similar to those in Wu and Wang (2008), and Ganti et al. (2014).

If we consider the spatial adjustment of sediment load shortly after the cutoff of sediment supply, we can further neglect the nonuniformity of the capacity (equilibrium) transport rate q_{se} along the channel, and Eq. (30) can be solved with a given upstream boundary condition. That is, with the boundary condition

$$q_s\big|_{x=0}=q_{sf} \tag{32}$$

Eq. (30) can be solved to yield

$$q_s=q_{se}+\left(q_{sf}-q_{se}\right)e^{-\frac{x}{L_{ad}}} \tag{33}$$

Here q_{sf} is the sediment supply rate per unit width at the upstream end. According to Eq. (33), q_s adjusts exponentially in space from q_{sf} to q_{se}, which also coincides with our simulation results in Section 3.1, as shown in Figs. 3-6. The adaptation length L_{ad} is the key parameter that controls the distance for q_s to approach the equilibrium sediment transport rate q_{se}. More specifically, q_s attains 1 - 1/e (i.e. 63.2%) of its adjustment from q_{sf} to q_{se} over a distance L_{ad}. Therefore, the larger the adaptation length, the slower q_s adjusts in space, so that the more evident lag effects and diffusivity are exhibited in the entrainment form. In the flux form, however, the sediment load responds simultaneously with the flow conditions, so that $L_{ad} = 0$ and $q_s = q_{se}$ along the entire channel reach.

For the case of uniform sediment in Section 3.1, $q_w = 6.67$ m^2/s and r_o is specified as unity. Therefore, the value of L_{ad} is determined only by the sediment fall velocity v_s. Figure 9 shows the value of the adaptation length L_{ad} for various sediment grain sizes, with the sediment fall velocity v_s calculated by the relation of Dietrich (1982). From the figure we can see that L_{ad} decreases sharply with the increase of grain size, indicating that the lag effects between sediment transport and flow conditions are evident for very fine sediment but gradually disappear when sediment is sufficiently coarse. For the sediment grain size of 65 μm implemented in Section 3.1, the corresponding $L_{ad} = 1.88$ km, which is much smaller than the 200 km reach of the computational domain. In this case and in general, ~~Therefore,~~ the predictions of the flux form and the entrainment form show little difference when $L_{ad}/L << 1$, where L is domain length. However, if we arbitrarily multiply the sediment fall velocity by a factor of 0.05, then L_{ad} becomes 37.60 km. With such a large adaptation length, it is no surprise that the entrainment form gives very different predictions from the flux form.

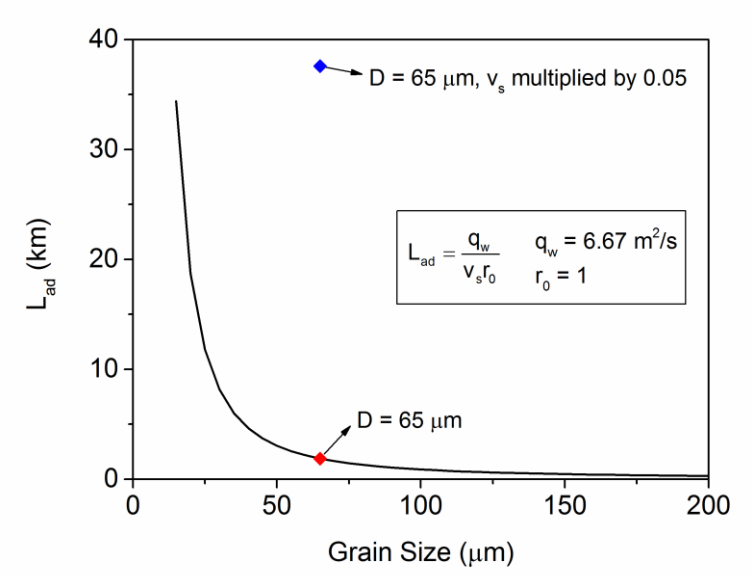

Figure 9. Relation between adaptation length L_{ad} and grain size D. The values of flow discharge per unit width q_w and recovery coefficient r_0 are the same as those in Section 3.1. The relation of Dietrich (1982) is implemented for sediment fall velocity.

The evolution of bed elevation z_b can also be affected by the value of L_{ad}. For example in the case of uniform sediment in Section 3.1, the flux form corresponds to an adaption length of zero. As a result, the flux form yields a spatial derivative of q_s near the upstream end that is relatively large, thus leading to fast degradation from the upstream end. In the case of the entrainment form, however, the spatial derivative of q_s is small with a large L_{ad}, thus leading to a slower and more diffusive bed degradation. This is especially evident when we arbitrarily reduce the sediment fall velocity by a factor of 0.05, while keeping grain size invariant.

The above analysis also holds for sediment mixtures, except that each grain size range will have its own adaptation length. Here we neglect the temporal derivative in Eq. (29) and analyze only the spatial adjustment of sediment load. If we neglect the spatial derivative in Eq. (29) and conduct a similar analysis for sediment concentration, we would find that the temporal adjustment of sediment concentration is also described by an exponential function of time, in analogy to Eq. (33).

4.2 Patterns of grain sorting: advection vs. diffusion

In Section 3.2 we find that the flux form and entrainment form of the Exner equation provide very different patterns of grain sorting for sediment mixtures: kinematic sorting waves are evident in the flux form but are diffused out in the entrainment form. The diffusivity of grain sorting becomes smaller and the kinematic waves appear, however, if we arbitrarily increase the sediment fall velocity by a factor of 20. In this section, we explain this behavior by analyzing the governing equations.

First we rewrite the sediment transport relation of Naito et al. (accepted subject to revision) in the following form,

$$q_{sei} = F_i q_{ri} \tag{34}$$

$$q_{ri} = \frac{u_*^{\,3}}{RgC_f} A_i \left(\tau_g^* \frac{D_g}{D_i} \right)^{B_i} \tag{35}$$

Substituting Eq. (34) into Eq. (6), which is the governing equation for surface fraction F_i in the flux form, we get

$$\frac{1}{I_f}\left(1-\lambda_p\right)\left[L_a \frac{\partial F_i}{\partial t} + \left(F_i - f_{Ii}\right)\frac{\partial L_a}{\partial t} \right] = f_{Ii} \frac{\partial \sum_{j=1}^{n} F_j q_{rj}}{\partial x} - \frac{\partial F_i q_{ri}}{\partial x} \tag{36}$$

Equation (36) can be written in the form of a kinematic wave equation with source terms as below,

$$\frac{\partial F_i}{\partial t} + c_{Fi} \frac{\partial F_i}{\partial x} = SF_i \tag{37}$$

$$c_{Fi} = \frac{I_f q_{ri}}{\left(1-\lambda_p\right) L_a}\left(1- f_{Ii}\right) \tag{38}$$

$$SF_i = -\frac{I_f F_i \left(1- f_{Ii}\right)}{\left(1-\lambda_p\right) L_a}\frac{\partial q_{ri}}{\partial x} + \frac{I_f f_{Ii}}{\left(1-\lambda_p\right) L_a}\frac{\partial \sum_{j=1}^{n, j\neq i} F_j q_{rj}}{\partial x} - \frac{F_i - f_{Ii}}{1-\lambda_p}\frac{\partial L_a}{\partial t} \tag{39}$$

where c_{Fi} is the i-th celerity of kinematic wave and SF_i denotes source terms. Since the surface geometric mean grain size D_{sg}, the total sediment load per unit width q_{sT} (which equals the equilibrium sediment transport rate q_{seT}), and the geometric mean grain size of sediment load D_{lg} are all closely related to the surface grain size fractions F_i, the evolution of these three parameters shows~~exhibit~~ marked advective behavior when simulated by the flux form of the Exner equation. However, the evolution of bed elevation z_b is related to~~with~~ $\partial q_{sT}/\partial x$, which is dominated by diffusion if q_{sT} is predominantly slope-dependent (as is the case here). The advection-diffusion character of the flux form of Exner equation for sediment mixtures has been documented thoroughly in a series of papers (e.g. Stecca et al., 2014; Stecca et al., 2016; An et al., 2017). The reader~~Readers~~ can reference these papers for more details.

Now we turn to the entrainment form of the Exner equation. Combined with the sediment transport rate per unit width $q_{si} = huC_i = q_wC_i$ and the dimensionless entrainment rate $E_i = r_{0i}q_{sei}/q_w$, Eq. (16) and Eq. (15) can be written as,

$$\frac{1}{I_f}\frac{\partial\left(\frac{q_{si}}{u}\right)}{\partial t} + \frac{\partial q_{si}}{\partial x} = \frac{v_{si} r_{oi}}{q_w}\left(q_{sei} - q_{si}\right) \tag{40}$$

$$\frac{1}{I_f}\left(1-\lambda_p\right)\left[L_a\frac{\partial F_i}{\partial t} + \left(F_i - f_{Ii}\right)\frac{\partial L_a}{\partial t}\right] = f_{Ii}\sum_{j=1}^{n}\frac{v_{sj} r_{0j}}{q_w}\left(q_{sej} - q_{sj}\right) - \frac{v_{si} r_{0i}}{q_w}\left(q_{sei} - q_{si}\right) \tag{41}$$

where Eq. (40) denotes the conservation of suspended sediment and Eq. (41) denotes the conservation of bed material. If we rewrite Eq. (40) in the following form,

$$q_{si} = q_{sei} - \frac{q_w}{v_{si} r_{oi}}\left[\frac{1}{I_f}\frac{\partial\left(\frac{q_{si}}{u}\right)}{\partial t} + \frac{\partial q_{si}}{\partial x}\right] \tag{42}$$

then q_{si} can be solved iteratively. With an initial guess of $q_{si} = q_{sei}$ and neglecting the temporal derivatives, we obtain the second order solution of q_{si} as,

$$q_{si} = q_{sei} - \frac{q_w}{v_{si} r_{oi}} \frac{\partial}{\partial x}\left(q_{sei} - \frac{q_w}{v_{si} r_{oi}} \frac{\partial q_{sei}}{\partial x} \right) \quad (43)$$

Details of the iteration scheme are given in ~~Appendix B~~Section S4 of the Supplement ~~Information~~.

Substituting Eq. (43) and Eq. (34) into Eq. (41), we find that

$$\frac{1}{I_f}\left(1-\lambda_p\right)\left[L_a \frac{\partial F_i}{\partial t} + \left(F_i - f_{Ii}\right)\frac{\partial L_a}{\partial t} \right] = f_{Ii} \sum_{j=1}^{n} \frac{\partial}{\partial x}\left(F_j q_{rj} - \frac{q_w}{v_{sj} r_{oj}} \frac{\partial F_j q_{rj}}{\partial x} \right) - \frac{\partial}{\partial x}\left(F_i q_{ri} - \frac{q_w}{v_{si} r_{oi}} \frac{\partial F_i q_{ri}}{\partial x} \right) \quad (44)$$

Expanding out the last two terms in Eq. (44) using the chain rule, after some work the relation for the conservation of bed material can be expressed as,

$$\frac{\partial F_i}{\partial t} + c_{Ei} \frac{\partial F_i}{\partial x} - \nu_i \frac{\partial^2 F_i}{\partial x^2} = SE_i \quad (45)$$

$$c_{Ei} = \frac{\left(1-f_{Ii}\right) I_f}{\left(1-\lambda_p\right) L_a}\left(q_{ri} - 2\frac{q_w}{v_{si} r_{0i}} \frac{\partial q_{ri}}{\partial x} \right) \quad (46)$$

$$\nu_i = \frac{\left(1-f_{Ii}\right) I_f q_w q_{ri}}{\left(1-\lambda_p\right) L_a v_{si} r_{0i}} \quad (47)$$

$$SE_i = \frac{I_f f_{Ii}}{\left(1-\lambda_p\right) L_a} \sum_{j=1}^{n, j\neq i} \frac{\partial}{\partial x}\left(F_j q_{rj} - \frac{q_w}{v_{sj} r_{oj}} \frac{\partial F_j q_{rj}}{\partial x} \right) - \frac{\left(1-f_{Ii}\right) I_f}{\left(1-\lambda_p\right) L_a}\left(F_i \frac{\partial q_{ri}}{\partial x} - \frac{q_w}{v_{si} r_{oi}} F_i \frac{\partial^2 q_{ri}}{\partial x^2} \right) - \frac{F_i - f_{Ii}}{L_a} \frac{\partial L_a}{\partial t} \quad (48)$$

where c_{Ei} is the celerity of kinematic wave, ν_i is the diffusivity coefficient, and SE_i denote source terms.

From Eq. (45) we can see that the governing equation for F_i in the entrainment form is an advection-diffusion equation, rather than the kinematic wave equation of the flux form. The surface geometric mean grain size D_{sg} is governed by Eq. (45), with describes the variation of the surface fractions F_i from which it is computed. The equilibrium sediment transport rate q_{sei} is governed by Eq. (45) because we implement a surface-based sediment transport relation as shown in Eq. (34). According to Eq. (43), the total sediment load per unit width q_{sT} and the geometric mean grain size of sediment load D_{lg} must also be closely related to the surface grain size fractions F_i. Therefore, the diffusion terms in Eq. (45) can lead to ~~the~~ dissipation of the kinematic waves in Figs. 7(b), 7(c), and 7(d).

From Eq. (47), we can also see that the diffusivity coefficient ν_i is related to the sediment fall velocity v_{si}: the larger the sediment fall velocity, the smaller the diffusivity coefficient. Thus when we increase the sediment fall velocity arbitrarily by a factor of 20 in Section 3.2, the kinematic waves become more evident as a result of the reduction of diffusivity.

Moreover if we compare the celerity of kinematic waves in both the flux form and the entrainment form, we have

$$\frac{c_{Ei}}{c_{Fi}} = 1 - r_{ci} \tag{49}$$

$$r_{ci} = 2\frac{L_{adi}}{q_{ri}}\frac{\partial q_{ri}}{\partial x} \tag{50}$$

where L_{adi} is the adaptation length for the i-th size range as defined by Eq. (31). More specifically, the value of r_{ci} depends on $\partial q_{ri}/\partial x$. For our numerical simulation in Section 3.2, $\partial q_{ri}/\partial x > 0$ as a result of bed degradation progressing from the upstream end, thus leading to a positive value of r_{ci} and an entrainment celerity c_{Ei} that is smaller than the corresponding flux celerity c_{Fi}. This is consistent with our numerical results: the kinematic waves in Fig. 8 predicted by the entrainment form are somewhat smaller than the kinematic waves in Fig. 6 predicted by the flux form.

4.3 Modeling implications and limitations

In Section 3, two numerical cases are conducted to compare the flux form and the entrainment form of the Exner equation, but only within 0.2 year after the cutoff of sediment supply. Here we run both numerical cases for a longer time (5 years). Table 4 shows the results of the case of uniform sediment (as described in Section 3.1) within 5 years, and Table 5 shows the results of the case of sediment mixtures (as described in Section 3.2) within 5 years. For both cases, the δ values, corresponding to relative deviation between the flux and entrainment forms, become quite small after 1 year, thus validating our assumption that the predictions of the two forms tend to be most evident shortly after disruption, but gradually diminish over a longer time scale. Moreover, if the water and sediment supply are kept constant for a sufficiently long time, the flux form and entrainment form of Exner equation predict exactly the same equilibrium, in terms of both the channel slope and the bed surface texture~~,~~. ~~u~~Under such conditions, ~~which~~ the sediment transport rate (of each size range) equals to the equilibrium sediment transport rate (of each size range), and also equals to the sediment supply rate (of each size range).

Table 4. Quantification of the difference between predictions of the flux form and the entrainment form in the case of uniform sediment. The maximum δ in the calculational domain are presented for each of 5 years.

		1 yr	2 yr	3 yr	4 yr	5 yr
original v_s	$\delta(z_b)$	~~2.97~~3.0 %	2.~~67~~ 7 %	2.~~56~~ 6 %	2.5~~4~~ %	2.~~55~~ 6 %
	$\delta(q_s)$	~~2.97~~3.0 %	1.~~77~~ 8 %	1.3~~1~~ %	1.~~09~~ 1 %	1.0~~0~~ %

Table 5. Quantification of the difference between predictions of the flux form and the entrainment form in the case of sediment mixtures. The maximum δ in the calculational domain are presented for each of five years.

		1 yr	2 yr	3 yr	4 yr	5 yr
original v_s	$\delta(z_b)$	2.~~16~~2 %	1.~~85~~9 %	1.7~~4~~ %	1.7~~0~~ %	1.7~~1~~ %
	$\delta(q_{sT})$	2.9~~0~~ %	1.8~~4~~ %	1.5~~1~~ %	1.4~~0~~ %	3.~~89~~9 %
	$\delta(D_{sg})$	5.2~~2~~ %	3.9~~3~~ %	3.5~~4~~ %	4.7~~4~~ %	3.9~~2~~ %
	$\delta(D_{lg})$	0.7~~6~~ %	0.6~~1~~ %	~~0.96~~1.0 %	1.3~~4~~ %	0.8~~2~~ %

Based on the numerical modeling and mathematical analysis in this paper, we ~~summarize below the circumstances under which the entrainment form of the Exner equation might be required.~~ suggest that the entrainment form of the Exner equation ~~to~~ be used when studying the river morphodynamics of fine-grained sediment (or more specifically sediment with small fall velocity). This is because the adaptation length L_a and the diffusivity coefficient ν_i are large for fine sediment, but the flux form of the Exner equation does not account for~~cannot consider the~~ lag effects or diffusivity of individual size fractions, thus leading to unrealistic simulation results. Such unrealistic simulation results can include an overestimation of advection as sediment sorts~~in terms of the sorting processes~~ (as shown in the case of sediment mixtures) and an overestimation of the aggradation/degradation rate (as shown in the case of uniform sediment) when sufficiently small grain sizes (or sediment fall velocities~~y~~) are considered. It should be noted, however, that~~Moreover, (1) T~~the difference in the predictions of the two forms of ~~the~~ Exner equation tends to be large shortly after disruption, but gradually diminishes over time. ~~Therefore, we suggest that the entrainment form of Exner equation should be used at short time scale (e.g., within a flood event), but that the flux form of Exner equation is applicable to long term river morphodynamics (e.g., more than one year). (2) The entrainment form of the Exner equation is necessary if sorting processes are to be studied. The flux form of Exner equation cannot consider the lag effects and diffusivity of individual size fractions, and therefore will result in an overestimation of the effect of advection on sorting processes. (3) The entrainment form of the Exner equation is necessary when dealing with fine-grained sediment (or more specifically sediment with small fall velocity), since the adaptation length L_a and the diffusivity coefficient ν_i are large under such circumstances.~~ The flux form of the Exner equation, on the other hand, is particularly applicable for coarse sediment, or when the sediment transport is dominated by bedload (e.g. gravel-bed rivers). The above results could have practical implications in regard to a wide range of issues including dam construction, water and sediment regulation, flood management, and ecological restoration schemes. The results can also be used as a reference for other fine-grained fluvial systems similar to the LYR, such as the Pilcomayo River in Paraguay/Argentina, South America (Martín-Vide et al., 2014).

It should be noted that in the morphodynamic models of this paper, we implement the mass and momentum conservation equations for clear water (i.e., Eq. (1) and Eq. (2)) to calculate flow hydraulics, instead of the mass and momentum equations for water-sediment mixture as suggested by Cao et al. (2004) and Cao et al. (2006). More specifically, Cui et al. (2005) have pointed out that when sediment concentration in the water is sufficiently small, bed elevation can be taken to be unchanging over characteristic hydraulic time scales, and the effects of flow-bed exchange on flow hydraulics can be neglected.

For the two simulation cases in this paper, the volume sediment concentration C drops from about 2×10^{-3} to about 2×10^{-4} in the case of uniform sediment, and from about 4×10^{-3} to about 4×10^{-4} in the case of sediment mixtures, due to the cutoff of sediment supply at the upstream end. These dilute concentrations validate our implementation of mass and momentum conservation equations for clear water. Our assumption is not necessarily correct for the entire Yellow River. Upstream of our study reach, and especially upstream of Sanmenxia Dam, the flow is often hyperconcentrated (Xu, 1999).

Considering the fact that in our numerical simulations a constant inflow discharge (along with a flood intermittency factor) is implemented, and also considering that the morphodynamic time scale is much larger than the hydraulic time scale in our case, the quasi-steady approximation or even the normal flow approximation can be introduced to further save computational efforts (Parker, 2004). But one thing that should be noted is that in our simulation results in Section 3, the bed exhibits an inverse slope near the upstream end. The normal flow assumption becomes invalid under such circumstances, so requiring a full unsteady shallow water model.

By definition, the recovery coefficient r_o is the ratio of the near-bed to the flux-depth-averaged concentration of suspended load, and is thus related to the concentration profile. In our simulation r_0 is specified as unity. That is, density stratification effects of suspended sediment are neglected, and the vertical profile of sediment concentration is regarded as uniform. However in natural rivers, the value of r_0 can vary significantly under different circumstances (Cao et al., 2004; Duan and Nanda, 2006; Zhang and Duan, 2011; Zhang et al., 2013). In general, the value of r_0 is no less than unity and can be as large as 12 (Zhang and Duan, 2011). Therefore according to our mathematical analysis in Section 4.1 and 4.2, $r_0 = 1$ corresponds to a maximum adaptation length L_{ad}, a maximum diffusivity coefficient ν_i, and a minimum ratio of celerities c_{Ei}/c_{Fi}, thus leading to the largest difference between the flux form and the entrainment form. When sediment concentration is sufficiently high, hindered settling effects reduce the sediment fall velocity. Considering the fact that the sediment concentrations considered in our simulation are fairly small, hindered settling effects are not likely significant. More study on stratification and hindered settling effects would be useful~~are merited~~ in the case of the LYR.

In this paper, a one-dimensional morphodynamic model with several simplifications is implemented to compare the flux-based Exner equation and the entrainment-based Exner equation in context of the LYR. However, a~~the~~ site-specific model of the morphodynamics of the LYR without these simplifications would be much more complex. For example, in our 1D simulation we observe bed degradation after the closure~~operation~~ of the Xiaolangdi Dam, but we cannot resolve its structure in the lateral direction. In natural rivers, ~~however,~~ bed degradation is generally~~mostly~~ not uniform across the channel width, but may be ~~could~~ concentrated in the thalweg. Moreover, the spatial variation of channel width and initial slope, which are not considered in this paper, are also important when considering applied~~certain~~ problems. The above-mentioned issues~~problems~~, even though not the aim of this paper, ~~could~~ merit future research (e.g. He et al., 2012). Besides, Chavarrias et al. (2018) have reported that morphodynamic models considering mixed grain sizes may be subject to numerical instabilities that are not easily remedied. No such instabilities were encountered in the present work.

5 Conclusion

In this paper, we compare two formulations for sediment mass conservation in context of the Lower Yellow River, i.e. the flux form of the Exner equation and the entrainment form of the Exner equation. In the flux form of the Exner equation, the conservation of bed material is related to the streamwise gradient of sediment transport rate, which is in turn computed based on the quasi-equilibrium assumption according to which the local sediment transport rate equals the capacity rate. In the entrainment form of the Exner equation, on the other hand, the conservation of bed material is related to the difference between the entrainment rate of sediment from the bed into the flow and the deposition rate of sediment from the flow onto the bed. A nonequilibrium sediment transport formulation is applied here, so that the sediment transport rate can lag in space and time behind changing flow conditions. Despite the fact that the entrainment form is usually recommended for the morphodynamic modeling of the LYR due to its fine-grained sediment, there has been little discussion of the differences in predictions between the two forms.

Here we implement a 1-D morphodynamic model for this problem. The fully unsteady Saint Venant Equations are implemented for the hydraulic calculation. Both the flux form and the entrainment form of Exner equation are implemented for sediment conservation. For each formulation, we include the options of both uniform sediment and sediment mixtures. Two generalized versions of the Engelund-Hansen relation specifically designed for the LYR are implemented to calculate the quasi-equilibrium sediment transport rate (i.e., sediment transport capacity). They are the version of Ma et al. (2017) for uniform sediment, and the version of Naito et al. (accepted subject to revision) for sediment mixtures. The method of Viparelli et al. (2010) is implemented to store and access bed stratigraphy as the bed aggrades and degrades. We apply the morphodynamic model to two cases with conditions typical of the LYR.

In the first case, a uniform bed material grain size of 65 μm is implemented. We study the effect of cutoff of sediment supply, as occurred after the operation of Xiaolangdi Dam in 1999. We find that the flux form and the entrainment form give very similar predictions for this case. Through quantification of the difference between the two forms with a normalized measure of relative difference, we find that difference in the prediction of bed elevation is quite small (< 4%), but difference in the prediction of sediment load can be relatively large (about 20%) shortly after the cutoff of sediment supply. ~~Moreover, the predictions of the entrainment form become very different from those of the flux form if we arbitrarily reduce the sediment fall velocity by a multiplicative factor of 0.05, while keeping grain size unchanged.~~

The results for the case of uniform sediment can be explained by analyzing the governing equation of sediment load q_s. In the flux form, the volume sediment transport rate per unit width q_s ~~=~~ equals to the local equilibrium (capacity) value q_{se}. ~~I~~But in the entrainment form, however, we find that the difference between q_s and q_{se} decays exponentially in space. The adaptation length $L_{ad} = q_w / (v_s r_0)$ is the key parameter that controls the distance for q_s to approach its equilibrium value q_{se}. The larger the adaptation length, the more different the predictions of the two forms will be. For computational conditions in this case, the adaption length is relatively small (L_{ad} = 1.88 km)~~, but it becomes much larger (L_{ad} = 37.6 km) if sediment fall velocity is arbitrarily divided by a factor of 20~~.

In the second case the bed material consists of mixtures ranging from 15 μm to 500 μm. We find that the flux form and the entrainment form give very different patterns of grain sorting. Evident kinematic waves occur at various timescales in the flux form, but no evident kinematic waves can be observed in the entrainment form. The different sorting patterns are reflected in the evolution of surface geometric mean grain size D_{sg}, total sediment load q_{sT} and geometric mean grain size of sediment load D_{lg}, but are not reflected in the evolution of bed elevation z_b. ~~Kinematic waves appear in the entrainment form if we arbitrarily increase the sediment fall velocity by multiplying a factor of 20 without changing the grain size. This large increase in fall velocity leads to a large decrease in adaptation length, so that the entrainment form behaves much more like the flux form. This notwithstanding, the kinematic waves are still more diffusive and slower than those predicted by the flux form.~~

The different sorting patterns exhibited in the case of sediment mixtures can be explained by analyzing the governing equation for bed surface fractions F_i, i.e. the grain size-specific conservation of bed material. We find that in the flux form, the governing equation for F_i can be written in the form of a kinematic wave equation. In the entrainment form, however, the governing equation for F_i is an advection-diffusion equation. It is the diffusion term which ~~can~~ leads to the dissipation of kinematic waves. Moreover, in the advection-diffusion equation arising from the entrainment form, the coefficient of diffusivity is inversely proportional to the sediment fall velocity. In addition, under the condition of bed degradation the wave celerity is smaller than that ~~celerity~~ arising from the flux form.

Overall, our results indicate that the more complex entrainment form of the Exner equation might be required ~~under the following circumstances~~when the sorting processes of ~~the~~ fine-grained sediment (or sediment with small fall velocity) is ~~to be~~ studied, especially at~~in~~ relatively short timescale. Under such circumstances, the flux form of the Exner equation might overestimate ~~the~~ advection in sorting processes as well as the aggradation/degradation rate, due to the fact that it cannot account for~~consider~~ the relatively large adaptation length or diffusivity of fine particles.

~~: (1) when short-term (e.g., within a flood event) river morphodynamics is considered; (2) when sorting processes are studied; and (3) when fine-grained sediment (or more specifically sediment with small fall velocity) is considered.~~

~~Appendix A: Comparison of two relations for sediment fall velocity: Dietrich (1982) against Ferguson and Church (2004)~~

~~In this paper, we implement the relation of Dietrich (1982) to calculate sediment fall velocity v_s. The relation is,~~

$$v_s = R_f \sqrt{RgD} \quad \text{(A1)}$$

$$\ell n\left(R_f\right) = -b_1 + b_2 \ell n\left(\mathrm{Re}_p\right) - b_3\left[\ell n\left(\mathrm{Re}_p\right)\right]^2 - b_4\left[\ell n\left(\mathrm{Re}_p\right)\right]^3 + b_5\left[\ell n\left(\mathrm{Re}_p\right)\right]^4 \quad \text{(A2)}$$

$$\mathrm{Re}_p = \frac{\sqrt{RgDD}}{\nu} \quad \text{(A3)}$$

where $b_1 = 2.891394$, $b_2 = 0.95296$, $b_3 = 0.056835$, $b_4 = 0.002892$, $b_5 = 0.000245$, and $\nu = 10^{-6}$ is the kinematic viscosity of water.

Another widely used relation for sediment fall velocity is the relation of Ferguson and Church (2004), which is regarded as applying to nearly the entire range of viscous to turbulent conditions.

$$v_s = \frac{RgD^2}{C_1\nu + \left(0.75C_2RgD^3\right)^{0.5}} \quad \text{(A4)}$$

where $C_1 = 18$ and $C_2 = 0.4$ for smooth spheres; $C_1 = 18$ and $C_2 = 1.0$ for sieve diameters of natural sand; and $C_1 = 20$ and $C_2 = 1.1$ for nominal diameters of natural sand. More specifically, the relation of Ferguson and Church (2004) converges on Stokes' law for small grains, and to a constant drag coefficient for large grains.

Considering the fact that the sediment of LYR is finer than most sand bed rivers (Ma et al., 2017), here we compare the two relations for sediment fall velocity in the context of the LYR. The two parameters in Ferguson and Church are specified as $C_1 = 18$ and $C_2 = 1.0$. In our simulation, the sediment size range of the LYR is specified as 15 μm ~ 500 μm.

According to Fig. A1, the relation of Dietrich (1982) and the relation of Ferguson and Church (2004) coincide with each other within this size range, thus justifying our implementation of Dietrich (1982) in the simulation. For grain sizes smaller than 15 μm, sediment becomes washload in the LYR and Dietrich (1982) predicts sediment fall velocities that are smaller than those predicted by Ferguson and Church (2004). For sediment coarser than 500 μm, Dietrich (1982) somewhat overestimates sediment fall velocity compared with Ferguson and Church (2004).

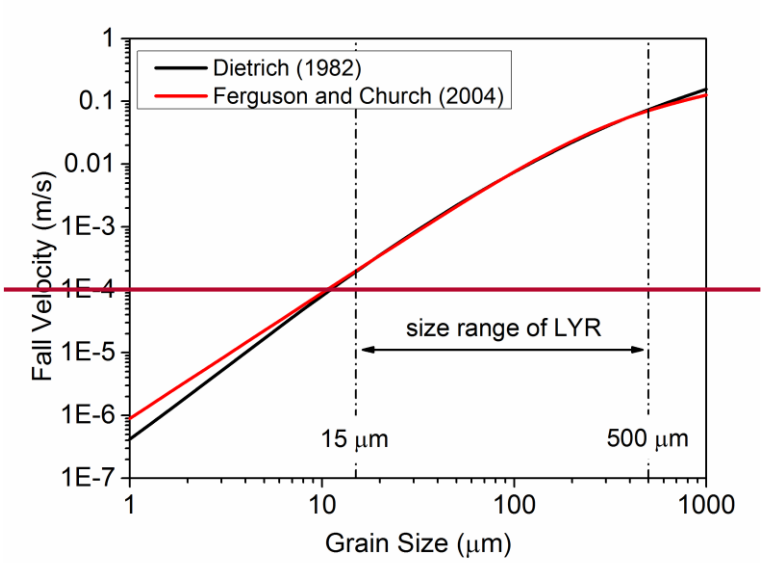

Figure A1. Comparison of two relations for sediment fall velocity: Dietrich (1982) and Ferguson and Church (2004)

Appendix B: Iterative solution of sediment transport rate q_{si} in the entrainment form

The parameter q_{si} in Eq. (40) is solved iteratively as below,

$$q_{si}^{(m+1)} = q_{sei} - \frac{q_w}{v_{si} r_{oi}} \left[\frac{1}{I_f} \frac{\partial \left(\frac{q_{si}^{(m)}}{u} \right)}{\partial t} + \frac{\partial q_{si}^{(m)}}{\partial x} \right] \tag{B1}$$

where the superscript denotes the order of iteration. The following zero-order solution is specified as an initial value;

$$q_{si}^{(0)} = q_{sei} \tag{B2}$$

From this we can get the first order and the second order solution,

$$q_{si}^{(1)} = q_{sei} - \frac{q_w}{v_{si} r_{oi}} \left[\frac{1}{I_f} \frac{\partial \left(\frac{q_{sei}}{u} \right)}{\partial t} + \frac{\partial q_{sei}}{\partial x} \right] \tag{B3}$$

$$q_{si}^{(2)} = q_{sei} - \frac{q_w}{v_{si} r_{oi}} \frac{1}{I_f} \frac{\partial}{\partial t} \frac{1}{u} \left\{ q_{sei} - \frac{q_w}{v_{si} r_{oi}} \left[\frac{1}{I_f} \frac{\partial \left(\frac{q_{sei}}{u} \right)}{\partial t} + \frac{\partial q_{sei}}{\partial x} \right] \right\} - \frac{q_w}{v_{si} r_{oi}} \frac{\partial}{\partial x} \left\{ q_{sei} - \frac{q_w}{v_{si} r_{oi}} \left[\frac{1}{I_f} \frac{\partial \left(\frac{q_{sei}}{u} \right)}{\partial t} + \frac{\partial q_{sei}}{\partial x} \right] \right\} \quad \text{(B4)}$$

The second order iterative solution in Eq. (B4) is tedious in form, but the only terms of importance on the right-hand side are the spatial derivatives. Therefore we drop the time derivatives for simplicity. This gives,

$$q_{si} = q_{sei} - \frac{q_w}{v_{si} r_{oi}} \frac{\partial}{\partial x} \left(q_{sei} - \frac{q_w}{v_{si} r_{oi}} \frac{\partial q_{sei}}{\partial x} \right) \quad \text{(B5)}$$

which corresponds to Eq. (41) as implemented in Section 4.2.

Notation

C depth-flux-averaged sediment concentration

C_f dimensionless bed resistance coefficient

C_z dimensionless Chezy resistance coefficient

c_b near-bed sediment concentration

c_E celerity of the kinematic wave corresponding to F_i in the entrainment form

c_{Fi} celerity of the kinematic wave corresponding to F_i in the flux form

D sediment grain size

E dimensionless entrainment rate of sediment

F_i volumetric fraction of surface material in the i-th size range

f_{Ii} volumetric fraction of sediment in the i-th size range exchanged across the surface-substrate interface

g gravitational acceleration

h water depth

I_f flood intermittency factor

L_a thickness of active layer

L_{ad} adaptation length of suspended load

p_{si} volumetric fraction of bed material load in the i-th size range

q_{ri} normalized sediment transport rate per unit width for the i-th size range, defined by Eq. (34)

q_s volumetric sediment transport rate per unit width

q_{se} equilibrium volumetric sediment transport rate (capacity) per unit width

q_{sf} sediment supply rate per unit width

q_w flow discharge per unit width

R submerged specific gravity of sediment

r_0 user-specified parameter denoting the ratio between the near-bed sediment concentration and the flux-averaged sediment concentration

S bed slope

t time

u depth-averaged flow velocity

u_* shear velocity

v_s sediment fall velocity

x streamwise coordinate

z_b bed elevation

α coefficient in Eq. (6) for interfacial exchange fractions

Δt_h time step for hydraulic calculation

Δt_m time step for morphologic calculation

Δx spatial step length.

δ normalized parameter quantifying the fraction difference between the entrainment form and the flux form.

λ_p porosity of bed deposit

ν_i diffusivity coefficient corresponding to F_i in the entrainment form;

ρ density of water

ρ_s density of sediment

τ_b bed shear stress

τ^* dimensionless shear stress (Shields number)

Competing interests

The authors declare that they have no conflict of interest.

Acknowledgments

The participation of Chenge An and Xudong Fu was made possible in part by grants from the National Natural Science Foundation of China (grants 51525901 and 91747207), and the Ministry of Science and Technology of China (grant 2016YFC0402406). The participation of Andrew J. Moodie, Hongbo Ma, Kensuke Naito, and Gary Parker were made possible

in part by grants from National Science Foundation (grant EAR-1427262). The participation of Yuanfeng Zhang was made possible in part by grant from the National Natural Science Foundation of China (grant 51379087). Part of this research was accomplished during Chenge An's visit in the University of Illinois at Urbana-Champaign, which was supported by the China Scholarship Council (file no. 201506210320). The participation of Andrew J. Moodie was also supported by an National Science Foundation Graduate Research Fellowship (grant 145068). We thank the Morphodynamics Class of 2016 at the University of Illinois at Urbana-Champaign for their participation in preliminary modeling efforts.

References

An, C., Cui, Y., Fu, X., and Parker, G.: Gravel-bed river evolution in earthquake-prone regions subject to cycled hydrographs and repeated sediment pulses, Earth Surface Processes and Landforms, 42, 2426-2438, doi:10.1002/esp.4195, 2017.

An, C., Fu, X., Wang, G., and Parker, G.: Effect of grain sorting on gravel bed river evolution subject to cycled hydrographs: Bed load sheets and breakdown of the hydrograph boundary layer, Journal of Geophysical Research-Earth Surface, 122, 1513-1533, doi:10.1002/2016JF003994.

Armanini, A. and Di Silvio, G.: A one-dimensional model for the transport of a sediment mixture in non-equilibrium conditions, Journal of Hydraulic Research, 26(3), 275-292, doi:10.1080/00221688809499212, 1988.

Bell, R. G. and Sutherland, A. J.: Nonequilibrium bedload transport by steady flows, Journal of Hydraulic Engineering, 109(3), 351-367, 1983.

Blom, A., Ribberink, J. S., and de Vriend, H. J.: Vertical sorting in bed forms: Flume experiments with a natural and a trimodal sediment mixture, Water Resources Research, 39(2), 1025, doi:10.1029/2001WR001088, 2003.

Blom, A.: Different approaches to handling vertical and streamwise sorting in modeling river morphodynamics, Water Resources Research, 44(3), W03415, doi:10.1029/2006WR005474, 2008.

Blom, A., Viparelli, E., Chavarr ás, V.: The graded alluvial river: profile concavity and downstream fining, Geophysical Research Letters, 43, 1–9, doi:10.1002/2016GL068898, 2016.

Blom, A., Arkesteijn, L., Chavarr ás, V., Viparelli, E.: The equilibrium alluvial river under variable flow and its channel-forming discharge, Journal of Geophysical Research-Earth Surface, 122, 1924-1948, doi: 10.1002/2017JF004213, 2017.

Bohorquez, P. and Ancey, C.: Particle diffusion in non-equilibrium bedload transport simulations, Applied Mathematical Modeling, 40(17-18), 7474-7492, doi:10.1016/j.apm.2016.03.044, 2016.

Bradley, B. R. and Venditti J G.: Reevaluating dune scaling relations, Earth-Science Reviews, 165, 356-376, 2017.

Brownlie, W. R.: Prediction of flow depth and sediment discharge in open channels, W. M. Keck Laboratory of Hydraulics and Water Resources, California Institute of Technology, Pasadena, USA, Rep. KH-R-43A, 232 pp., 1981.

Cao, Z., Pender, G., Wallis, S., and Carling, P.: Computational dam-break hydraulics over erodible sediment bed, Journal of Hydraulic Engineering, 130(7), 689-703, 2004.

Cao, Z., Pender, G., and Carling, P.: Shallow water hydrodynamic models for hyperconcentrated sediment-laden floods over erodible bed, Advances in Water Resources, 29(4), 546-557, doi:10.1016/j.advwatres.2005.06.011, 2006.

Chavarrás, V., Stecca, G., and Blom, A.: Ill-posedness in modeling mixed sediment river morphodynamics, Advances in Water Resources, 114, 219-235, doi:10.1016/j.advwatres.2018.02.011, 2018.

Cui, Y., Parker, G., Lisle T. E., Pizzuto, J. E., and Dodd, A. M.: More on the evolution of bed material waves in alluvial rivers, Earth Surface Processes and Landforms, 30, 107-114, doi:10.1002/esp.1156, 2005.

Dietrich, E. W.: Settling velocity of natural particles, Water Resources Research, 18(6), 1626-1982, doi:10.1029/WR018i006p01615, 1982.

Dorrell, R. M. and Hogg, A. J.: Length and time scales of response of sediment suspensions to changing flow conditions, Journal of Hydraulic Engineering, 138(5), 430-439, doi:10.1061/(ASCE)HY.1943-7900.0000532, 2012.

Duan, J. G. and Nanda, S. K.: Two-dimensional depth-averaged model simulation of suspended sediment concentration distribution in a groyne field, Journal of Hydrology, 324(3-4), 426-437, 2006.

Einstein, H. A.: Bedload transport as a probability problem, PhD thesis, Mitt. Versuchsanst. Wasserbau Eidg. Tech. Hochsch, Zurich, Switzerland, 1937.

El kadi Abderrezzak, K. and Paquier, A.: One-dimensional numerical modeling of sediment transport and bed deformation in open channels, Water Resources Research, 45, W05404, doi:10.1029/2008WR007134, 2009.

Engelund, F. and Hansen, E.: A monograph on sediment transport in alluvial streams, Technisk Vorlag, Copenhagen, Denmark, 1967.

Exner, F. M.: Uber die Wechselwirkung zwischen Wasser und Geschiebe in Flussen, Sitzber. Akad. Wiss Wien, 134(2a), 169-204, 1920, (in German).

Ferguson, R. I. and Church, M.: A simple universal equation for grain settling velocity, Journal of Sedimentary Research, 74(6), 933-937, doi:10.1306/051204740933, 2004.

Ganti, V., Lamb, M. P., and McElroy, B.: Quantitative bounds on morphodynamics and implications for reading the sedimentary record, Nature Communications, 5, 3298, doi:10.1038/ncomms4298, 2014.

Guan, M., Wright, N. G., and Sleigh, P. A.: Multimode morphodynamic model for sediment-laden flows and geomorphic impacts, Journal of Hydraulic Engineering, 141(6), doi:10.1061/(ASCE)HY.1943-7900.0000997, 2015

Guo, Q., Hu, C., and Takeuchi, K.: Numerical modeling of hyper-concentrated sediment transport in the lower Yellow River, Journal of Hydraulic Research, 46(5), 659-667, doi:10.3826/jhr.2008.3009, 2008.

Harten, A., Lax, P. D., and van Leer, B.: On upstream differencing and Godunov-type schemes for hyperbolic conservation laws, SIAM Review, 25(1), 35-61, 1983.

He, L., Duan, J. G., Wang G., and Fu, X.: Numerical simulation of unsteady hyperconcentrated sediment-laden flow in the Yellow River, Journal of Hydraulic Engineering, 138(11), 958-969, doi:10.1061/(ASCE)HY.1943-7900.0000599, 2012.

Hirano, M.: On riverbed variation with armoring, Proc. Jpn. Soc. Civ. Eng., 195, 55-65, 1971, (in Japanese).

Hoey, T. B. and Ferguson, R.: Numerical simulation of downstream fining by selective transport in gravel bed rivers: Model development and illustration, Water Resour. Res., 30(7), 2251–2260, doi:10.1029/94WR00556, 1994.

Ma, H., Nittrouer, J. A., Naito, K., Fu, X., Zhang, Y., Moodie A. J., Wang, Y., Wu, B., and Parker, G.: The exceptional sediment load of fine-grained dispersal systems: Example of the Yellow River, China, Science Advances, 3(5), e1603114, doi:10.1126/sciadv.1603114, 2017.

Martín-Vide, J. P., Amarilla, M., and Zárate, F. J.: Collapse of the Pilcomayo River, Geomorphology, 205(15), 155-163, 2014.

Meyer-Peter, E. and Müller, R.: Formulas for bed-load transport, in Proceeding of the 2nd IAHR Meeting, International Association for Hydraulic Research, 7-9 June 1948, Stockholm, Sweden, 39-64, 1948.

Milliman. J. D. and Meade, R. H.: World-wide delivery of river sediment to the oceans, The Journal of Geology, 91(1), 1-21, 1983.

Minh Duc, B. and Rodi, W.: Numerical simulation of contraction scour in an open laboratory channel, Journal of Hydraulic Engineering, 134(4), 367-377, doi:10.1061/(ASCE)0733-9429(2008)134:4(367), 2008.

Naito, K., Ma, H., Nittrouer, J., Zhang, Y., Wu, B., Wang, Y., and Parker, G.: Extended Engelund-Hansen type sediment transport relation for mixtures based on the sand-silt-bed Lower Yellow River, China, Journal of Hydraulic Research, accepted subject to revision, 2018.

National Research Council: River Science at the U.S. Geological Survey. Washington, DC: The National Academies Press, available at: https://doi.org/10.17226/11773, 2007.

Ni, J. R., Zhang, H. W., Xue, A., Wieprecht, S., and Borthwick, A. G. L.: Modeling of hyperconcentrated sediment-laden floods in Lower Yellow River, Journal of Hydraulic Engineering, 130(10), 1025-1032, 2004.

Paola, C., Heller, P. L., and Angevine, C. L.: The large-scale dynamics of grain-size variation in alluvial basins, I: Theory, Basin Research, 4, 73~90, 1992.

Parker, G.: 1D Sediment Transport Morphodynamics with Applications to Rivers and Turbidity Currents, available at: http://hydrolab.illinois.edu/people/parkerg//morphodynamics_e-book.htm, 2004.

Parker, G., Paola, C., and Leclair, S.: Probabilistic Exner sediment continuity equation for mixtures with no active layer, Journal of Hydraulic Engineering, 126(11), 818-826, 2000.

Phillips, B. C. and Sutherland A. J.: Spatial lag effects in bedload sediment transport, Journal of Hydraulic Research, 27(1), 115-133, doi:10.1080/00221688909499247, 1989.

Stecca, G., Siviglia, A., and Blom, A.: Mathematical analysis of the Saint-Venant-Hirano model for mixed-sediment morphodynamics, Water Resources Research, 50, 7563–7589, doi:10.1002/2014WR015251, 2014.

914 Stecca, G., Siviglia, A., and Blom, A.: An accurate numerical solution to the Saint-Venant-Hirano model for mixed-sediment
915 morphodynamics in rivers, Advances in Water Resources, 93(Part A), 39-61, doi:10.1016/j.advwatres.2015.05.022,
916 2016.
917 Toro, E. F.: Shock-capturing methods for free-surface shallow flows, John Wiley, 2001
918 Toro-Escobar, C. M., Parker, G., and Paola, C.: Transfer function for the deposition of poorly sorted gravel in response to
919 streambed aggradation, Journal of Hydraulic Research, 34(1), 35-53, doi:10.1080/00221689609498763, 1996.
920 Tsujimoto, T.: A probabilistic model of sediment transport processes and its application for erodible-bed problems, Ph.D.
921 thesis, Kyoto University, Kyoto, Japan, 1978, (in Japanese).
922 Van der Scheer, P., Ribberink, J. S., and Blom, A.: Transport formulas for graded sediment; Behaviour of transport formulas
923 and verification with data. Research Report 2002R-002, Civil Engineering, University of Twente, Netherlands, 2002.
924 Viparelli, E., Sequeiros, O. E., Cantelli, A., Wilcock, P. R., and Parker, G.: River morphodynamics with creation/consumption
925 of grain size stratigraphy 2: numerical model, Journal of Hydraulic Research, 48(6), 727-741,
926 doi:10.1080/00221686.2010.526759, 2010.
927 Wang, S., Fu, B., Piao, S., L ü, Y., Ciais, P., Feng, X., and Wang, Y.: Reduced sediment transport in the Yellow River due to
928 anthropogenic changes, Nature Geoscience, 9, 38-41, doi:10.1038/ngeo2602, 2016.
929 Wu, W. and Wang, S. S. Y.: One-dimensional modeling of dam-break flow over movable beds. Journal of Hydraulic
930 Engineering, 133(1), 48-58, 2007.
931 Wu, W. and Wang, S. S. Y.: One-dimensional explicit finite-volume model for sediment transport, Journal of Hydraulic
932 Research, 46(1), 87-98, 2008.
933 Wu, W., Vieira, D. A., and Wang, S. S. Y.: A 1-D numerical model for nonuniform sediment transport under unsteady flows
934 in channel networks, Journal of Hydraulic Engineering, 130(9), 914-923, doi:10.1061/(ASCE)0733-
935 9429(2004)130:9(914), 2004.
936 Xu, J.: Erosion caused by hyperconcentrated flow on the Loess Plateau of China, Catena, 36(1999), 1-19, 1999.
937 Zhang, H., Huang, Y., and Zhao, L: A mathematical model for unsteady sediment transport in the Lower Yellow River,
938 International Journal of Sediment Research, 16(2), 150-158, 2001.
939 Zhang, S. and Duan, J. G.: 1D finite volume model of unsteady flow over mobile bed, Journal of Hydrology, 405, 57-68,
940 doi:10.1016/j.jhydrol.2011.05.010, 2011.
941 Zhang, S., Duan, J. G., and Strelkoff T. S.: Grain-scale nonequilibrium sediment-transport model for unsteady flow, Journal
942 of Hydraulic Engineering, 139(1), 22-36, doi:10.1061/(ASCE)HY.1943-7900.0000645, 2013.